CHAPTER VI.B

Two-step nitrification model parameter identifiability

ABSTRACT

The calibration of the two-step nitrification model described in chapter VI.A would be very tedious if all the parameters had to be estimated. Moreover, from an identifiability point of view, not all the parameters could be reliably estimated using only short-term batch respirometric and titrimetric profiles and particular experiments would be required. This chapter examines each of the parameters of the model and decides which of them can be either calculated or assumed from the literature and which should be estimated. Finally a range of identifiable parameters is obtained which will be used for model calibration and validation in Chapter VI.E.

VI.B.1 Introduction

When calibrating a model, the quantity and quality of the output measurements available define which parameters can be identifiable or not. Model identifiability is the ability to obtain a unique parameter set able to describe accurately the behaviour of the system Dochain and Vanrolleghem (2001) distinguished two different kind of identifiability:

- Structural identifiability: assuming a certain number of outputs (without experimental error), can we obtain a unique set of parameter values that describe our system? This part deals with the model structure itself.

- Practical identifiability: assuming a model structurally identifiable, is the information contained in our experimental data enough for a reliable estimation of our parameters? This part deals with the quantity and quality of our experimental measurements.

Petersen (2000) studied both the structural and practical identifiability of the two-step nitrification model and demonstrated that several parameter combinations are identifiable with their OUR and Hydrogen Production (HP) measurement outputs. In this chapter, the practical identifiability of the two-step nitrification model is studied using OUR and HPR as measured outputs.

Thee aim of this thesis is to calibrate the biological nutrient removal models using only “common” measurements (i.e. DO and pH). Obviously, the more variables measured, the more parameters would be identifiable. For example, it was impossible to identify the parameters related to ammonia stripping without ammonia measurements in the gas phase. In the LFS respirometer setup there are 5 measures available: DO, pH, T, accumulated acid and accumulated base. From these values, only two different output variables can be calculated: OUR and HPR.

VI.B.2 Physical and chemical equilibrium constants

These parameters were obtained from the literature and were maintained constant as long as the operational conditions coincided with the conditions under which these parameters were estimated.

VI.B.2.1 H_2O EQUILIBRIUM

K_w : Proton/hydroxyl equilibrium constant for pure water. It was calculated through expression VI.B1:

$$\ln Kw = -1344.5/T - 22.4773 \cdot \ln T + 140.932 \quad \text{(Edwards, 1978)} \qquad \text{(VI.B1)}$$

For T=298K; pKw = 14.00

VI.B.2.2 NH_4^+-NH_3 EQUILIBRIUM

K_3 : ammonium/ammonia equilibrium constant:

pK_3=9.245 at 25ºC (Gapes *et al.*, 2003)
K_3 = exp(-6344/T) (Anthonisen *et al.*, 1976) (VI.B2)
for T=298K; $\underline{pK_3 = 9.246}$

k_3 : ammonium/ammonia rate constant. This constant has a high value because the equilibrium is very fast and there were no available values in the literature for it. Hence, either the equilibrium is despised (assumed instantaneous) or high values are used to obtain instantaneous equilibrium (k_3= 10^7 1/min). The latter may produce numerical problems when solving the system.

VI.B.2.3 HNO_2-NO_2^- EQUILIBRIUM

K_4 : nitrite/nitrous acid constant calculated through equation VI.B3:

K_4= exp(-2333/T) (Anthonisen *et al.*, 1976) (VI.B3)
For T= 298K; $\underline{pK_4 = 3.4}$

k_4 : nitrite/nitrous rate constant. Likewise k_3, k_4 has a very high value so either the equilibrium is despised (and considered instantaneous) or either a very high value is given to the constant (k_4= 10^7 1/min).

VI.B.2.4 H_2CO_3 – CO_3^{2-} EQUILIBRIUM

K_1: first acidity constant of the equilibrium between the carbonic acid (H_2CO_3*) and bicarbonate (HCO_3^-).This equilibrium has been deeply studied due to its importance in aerated aqueous systems. Many empirical expressions for K_1 estimation can be found in the literature for pure water, as for example:

ln K_1 = -1209231/T - 36.7816·lnT+ 235.482 (Edwards, 1978) (VI.B4)
For T=298K; pK_1 = 6.35
K_1 = exp (-11.582-918.9/T) (Spérandio and Paul, 1997) (VI.B5)
For T=298K; pK_1 = 6.37
pK_1 = -14.8435+3404.71/T+0.032786·T (Cai and Wang, 1998) (VI.B6)
For T=298K; pK_1 = 6.35

According to these equations, a value close to $\underline{pK_1=6.36}$ should be obtained. However, this constant required special attention since it is very sensitive when HPR is used as an output variable. In addition, pK_1 was highly influenced by the medium ionic strength since two anions were present in the equilibrium (HCO_3^- and H^+). In this thesis, the medium had a high ionic strength because of the high concentrations of sodium, nitrate and chloride ions. The sodium cation was added as sodium bicarbonate to control the pH in the pilot plant where the biomass was withdrawn from. The chloride entered with the feed because ammonium was added as ammonium chloride. Finally, the nitrate was present as it was the nitrification product. A deeper description of the pilot plant operational conditions and the feed used can be found in Chapter III.1.6.

Sin (2004) also observed that pK_1 could change because of ionic strength and demonstrated that low variations of this constant were amplified to high differences in HPR measurements. As the ionic strength effect on pK_1 is somehow difficult to predict, this variable is generally estimated.

K_2 : second acidity constant which controls the equilibrium between the bicarbonate (HCO_3^-) and the carbonate (CO_3^{2-}). This value has been calculated through any of the following expressions:

$$\ln K_2 = -12431/T - 35.4819 \cdot \ln T + 220.067 \quad \text{(Edwards, 1978)} \qquad \text{(VI.B7)}$$

For T=298K; $pK_2 = 10.33$

$$pK_2 = -6.498 + 2902.39/T + 0.02379 \cdot T \quad \text{(Cai and Wang, 1998)} \qquad \text{(VI.B8)}$$

For T=298K; $pK_2 = 10.33$

In this work, the value of $\underline{pK_2 = 10.33}$ has been used. As the pH in the reactor was generally controlled at 7.5, pK_2 had practically no effect on the system since almost the whole inorganic carbon was in bicarbonate form. Hence, it did not need correction by the ionic strength whereas the pH value was close to neutrality.

k_1 : carbonic acid / bicarbonate rate constant:

For T = 293 K; k_1= 0.016 1/s
for T = 298 K; $\underline{k_1 = 0.0018\ 1/s}$ (both from Spérandio and Paul, 1997)

k_2 : bicarbonate / carbonate equilibrium rate constant

For T = 293K; k_2 = 4600 L/mol/s
for T= 298K; $\underline{k_2 = 4800\ L/mol/s}$ (both from Spérandio and Paul, 1997)

VI.B.2.5 O_2 STRIPPING

k_La_{O2} : oxygen mass transfer constant. This value was estimated through the DO profile by means of a reaeration profile with a procedure originally developed by Bandyopadhay *et al.*, (1976). This procedure is detailed in Chapter III.1.1.

S_O* : oxygen saturation value. This value can be calculated experimentally by means of S_{OE} and OUR. It could also be approximated as the value in pure water which can be found tabulated depending on the temperature (Metcalf and Eddy, 1991). For example, for T=298K; S_O* = 8.5 mg O_2/L. However, the medium conductivity can decrease this value and the value for pure water may not be correct.

VI.B.2.6 CO_2 STRIPPING

k_La_{CO2} : carbon dioxide mass transfer constant. The value of this parameter was critical to link the CTR with the HPR and its measurement is not a straightforward issue, since it requires carbon dioxide measurements in the gas phase. To avoid these measurements, it is generally approximated as function of the k_La_{O2}, which is more easily estimated. Royce and Thornmill (1991) showed that the ratio between the two k_Las should be around unity (0.89-0.92). This seems logical since both components are in the same gas phase and, then, both have same interfacial area, the same solvent properties and the same agitation properties. Sperandio and Paul (1997) calculated both values at different stirring speed and they found ratios around 0.60 (k_La_{CO2}/k_La_{O2}) for high stirred bioreactors and for low stirred reactors they found values around 0.91. As this thesis is developed in reactors with particularly low k_La value, the k_La_{CO2} value is estimated using this ratio of 0.91. This value of 0.91 can be also deduced using the diffusivities of both gases [eq. VI.B9].

$$k_L a_{CO2} = \sqrt{D_{CO2}/D_{O2}} \cdot k_L a_{O2} \qquad \text{(VI.B9)}$$

where D_i corresponds to the diffusivity of the compound i.

S_{CO2}^* : carbon dioxide saturation value. The physical equilibrium between the gas and liquid phases for CO_2 can be described according to expression VI.B10:

$$y_{CO2} \cdot P \cdot \Phi_{CO2} = H \cdot \gamma_{CO2} \cdot m_{CO2} \qquad \text{(VI.B10)}$$

where y_{CO2} = carbon dioxide molar fraction in the gas
P = gas pressure
Φ_{CO2} = carbon dioxide fugacity coefficient
H = Henry's constant
γ_{CO2} = carbon dioxide activity coefficient
m_{CO2} = CO_2 molality

Under biological conditions (i.e. atmospheric pressures and diluted solutions) expression VI.B10 can be simplified as:

$$y_{CO2} \cdot P = H \cdot M_{CO2} \qquad \text{(VI.B11)}$$

where H in the literature can be calculated through different equations

$H = 101.33 \cdot \exp(11.549 - 2440.4/T_L)$ Pa·m^3/mol (Minkevich and Neubert, 1985) (VI.B12)
For T=298; H=0.0283 Pa·m^3/mol
$H = \exp(11.25 - 395.9/(T - 175.9))$ Pa·m^3/mol (Schumpe *et al.*, 1982) (VI.B13)
For T=298; H=0.0291 Pa·m^3/mol
H = 0.034 M/atm at 298 K (Stumm and Morgan, 1996)

Some authors consider that the concentration of S_{CO2} in the gas phase does not vary much from the concentration in the inlet. In this case, S_{CO2}^* = $pCO_2^{IN} \cdot H$ (Sin, 2004). Figure VI.B1 shows ten hours of CO_2 measurements in air as a molar percentage of CO_2 in air. The mean obtained (solid line) is 0.0359, and the standard deviation calculated is 0.0022. The dotted lines show the value of the mean plus/minus twice the standard deviation. In this work, pCO_2^{IN} is considered 0.036 %. The same value of CO_2 percentage in air was described in Wett and Rauch (2002) or Royce and Thornhill (1991).

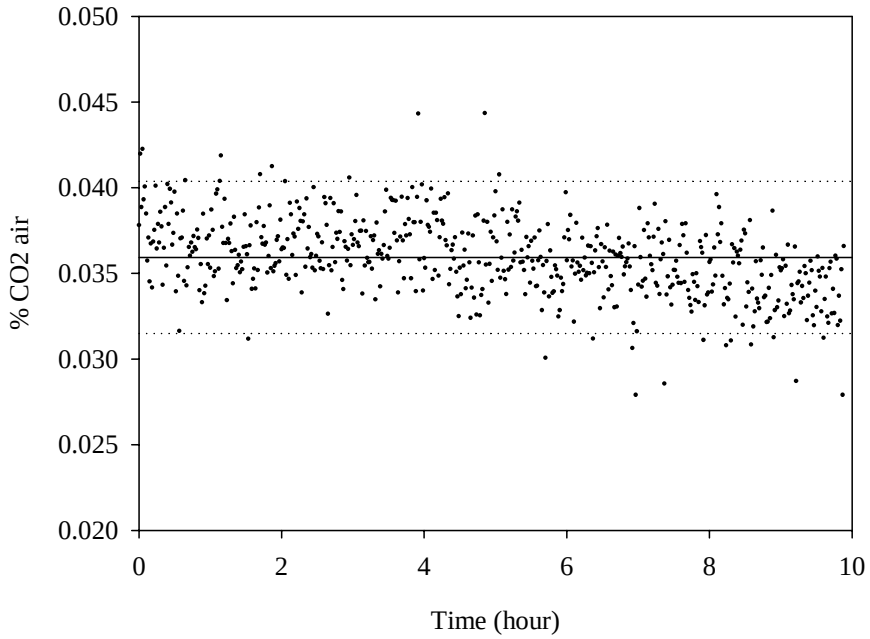

Figure VI.B1 CO_2 measurements in air (dotted) to estimate the mean (solid line) and the reliability in terms of 2·std dev (dotted line)

VI.B.2.7 NH_3 STRIPPING

k_La_{NH3} : ammonia mass transfer constant. Ammonia is much lower volatile than carbon dioxide (Kathesis *et al.*, 1998). Musvoto *et al.* (2000a,b) argued that the stripping rate for ammonia was two orders of magnitude lower than the carbon dioxide stripping. According to the values presented in these works k_La_{NH3} has been considered 0.01 k_La_{O2}. The ammonia stripping process is negligible in the pH working range of this thesis.

S_{NH3}* : ammonia saturation value. As the concentration of ammonia in air is zero, this value is also set to zero.

VI.B.2.8 OPERATIONAL CONDITIONS

ε_G : gas/liquid hold-up, stands for the fraction of the total two-phase volume which corresponds to the gas phase. This value was quite difficult to be experimentally calculated since the airflow was very low and the air bubbles were also very small. Hence, **ε_G** was also very low. Many empirical correlations exist as shown in Kantarci *et al.* (2005), which fundamentally link the ε_G with the superficial gas velocity and the physical properties of the medium such as density, viscosity, etc . Among all the correlations, with a wide range of complexity, the simplest one [eq. VI.B14] was chosen:

$$\varepsilon_G = \frac{u_G}{0.3 + 2 \cdot u_G} \quad \text{(Joshi and Sharma, 1979)} \qquad \text{(VI.B14)}$$

where u_G = superficial gas velocity (m/s)

VI.B.3 Biological parameters

These values are characteristic of each population and should not be assumed from the literature as long it is possible. They should be either estimated or calculated since they can be system specific.

VI.B.3.1 BIOMASS COMPOSITION: γ_X, i_{NB} AND v

γ_X : biomass degree of reduction (mol electron /mol C_X)
v : percentage of nitrogen in biomass (molar basis) (mols N /mols C_X)
i_{NB} : percentage of nitrogen in biomass (weight basis) (g N /g COD_X)

These parameters were experimentally measured with an elemental analysis of the biomass. According to the literature, a default biomass composition should be around $C_5H_7O_2N$ (Metcalf and Eddy, 1991), which corresponds to γx = 4, v = 0.2 and i_{NB}= 0.0875 gN/g COD_X. Table VI.B1 shows the experimental values obtained with 9 biomass samples which were very close to the theoretical values. The oxygen fraction could not be assessed with these experiments and, hence, the default value was assumed (i.e. 0.4 mol O_2/ mol C_X).

Hence, according to Table VI.B1, the biomass composition is: $C_{0.2}H_{1.54}O_{0.4}N_{0.18}$, which corresponds to **γx** = 4.2, **v** = 0.18 and **i_{NB}** = 0.075 g N /g COD_X

Table VI.B1 Elemental biomass composition

Parameter/Sample	1	2	3	4	5	6	7	8	9	Mean	Default
N(% weight)	6.07	5.86	5.82	6.03	5.88	5.65	5.75	5.68	5.89		
C (% weight)	28.96	28.53	28.33	27.5	28.3	26.68	27.63	27.32	28.23		
H(% weight)	3.77	3.66	3.6	3.48	3.62	3.34	3.71	3.47	3.71		
N (molar)	0.43	0.42	0.42	0.43	0.42	0.40	0.41	0.41	0.42		
C (molar)	2.41	2.38	2.36	2.29	2.36	2.22	2.30	2.28	2.35		
H (molar)	3.77	3.66	3.60	3.48	3.62	3.34	3.71	3.47	3.71		
N/C	0.18	0.18	0.18	0.19	0.18	0.18	0.18	0.18	0.18	0.179	0.2
C	1.00	1.00	1.00	1.00	1.00	1.00	1.00	1.00	1.00	1.000	1
H/C	1.56	1.54	1.52	1.52	1.53	1.50	1.61	1.52	1.58	1.544	1.4

VI.B.3.2. SUBSTRATE LIMITATION CONSTANTS

K_{OA} : oxygen affinity constant for nitritation (mg O_2/L)
K_{ON} : oxygen affinity constant for nitratation (mg O_2/L)
$K_{NH,A}$: Ammonium affinity constant of AOB (mg N-NH_4^+/L)
K_{NO} : Nitrite affinity constant (mg N-NO_2^-/L)

The substrate limitation constants are deeply discussed further in chapters VI.C (oxygen limitations), VI.D (inorganic carbon limitations) and VI.E (model calibration). The oxygen affinity constants are either assumed from the literature or omitted considering no oxygen limitations. However, the respirometric experiments in this thesis were often conducted under low k_La conditions and the DO in the reactor reached values where the limitation effect was not negligible. The values for the oxygen constants (chapter VI.C) were **K_{OA}** = 0.74 mg O_2/L i **K_{ON}** = 1.75 mg O_2/L. On the other hand, the values for $K_{NH,A}$ and K_{NO} were estimated because the range obtained in the literature is very wide.

VI.B.3.3 BIOMASS GROWTH YIELDS: Y_A AND Y_N

Y_A : AOB growth yield (g COD_X /g N)
Y_N : NOB growth yield (g COD_X /g N)

The existing correlation between the parameters of Monod kinetics (i.e. growth yield, the maximum growth rate and affinity constant) has already been described in the literature (e.g Holmberg, 1982; Baltes *et al.*, 1994; Versyck *et al.*, 1997; Petersen, 2000 or Liu and Zachara, 2001 among many others). Some authors propose modifications of the common batch experiments to maximise the reliability of the estimation of both parameters together such as fed-batch experiments (Munack and Posten, 1989; Baltes *et al.*, 1994).

Sensitivity functions are a valuable tool to study correlations between parameters, as did Holmberg (1982) for Michaelis–Menten parameters. The correlation of μ_{MAX} and Y is depicted in Figure VI.B2, which shows that sensitivity functions for both parameters for AOB and NOB with OUR as an output measurement. The identifiability problem can be easily observed since the two functions are almost proportional. This indicates that several parameter combinations of μ_{MAX} and Y would result in the same simulated OUR profile. Hence, one of them should be either estimated in a different experiment or assumed from the literature.

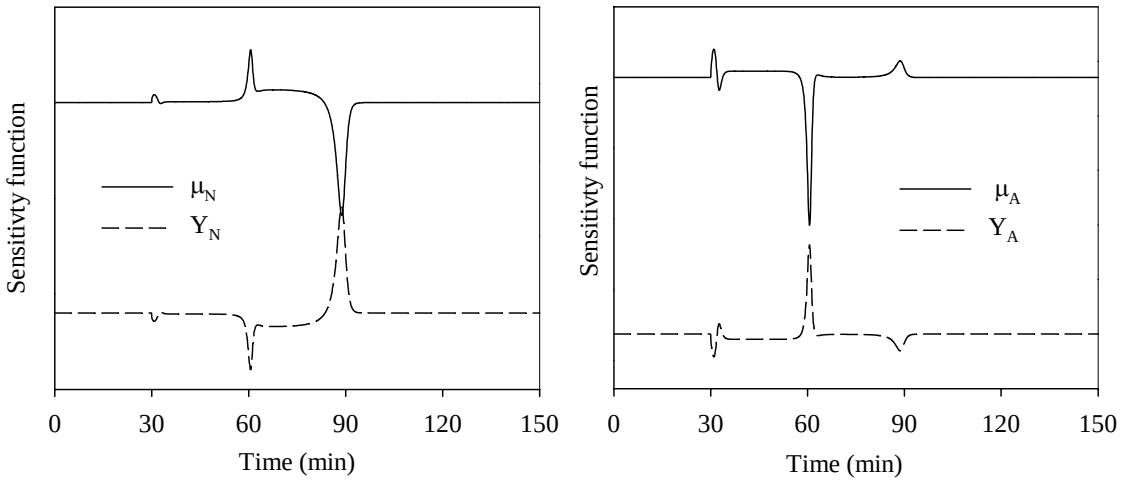

Figure VI.B2 Sensitivity functions for μ_M and Y_N (LEFT) and μ_A and Y_A (RIGHT) for an experiment with two pulses of 18.75 mg N-NH_4^+/L and 18.75 mg N-NO_2^-/L with OUR as a measured output.

Figure VI.B3 depicts the 3D contour graphics of the cost function around the optimum with OUR as the measured variable. A valley can be clearly observed which indicates a strong correlation between the two parameters is observed and, hence non-reliable estimates would be obtained.

Petersen (2000) also observed this problem and studied the structural identifiability of the two-step nitrification model considering respirometric and titrimetric data. Her theoretical study concluded that Y_A became uniquely identifiable only when both measurements were combined. Nevertheless, the titrimetric data could not theoretically solve the correlation between μ_{MAXN} and Y_N. Then, only Y_A could theoretically be estimated without any identifiability problem combining respirometric and titrimetric measurements.

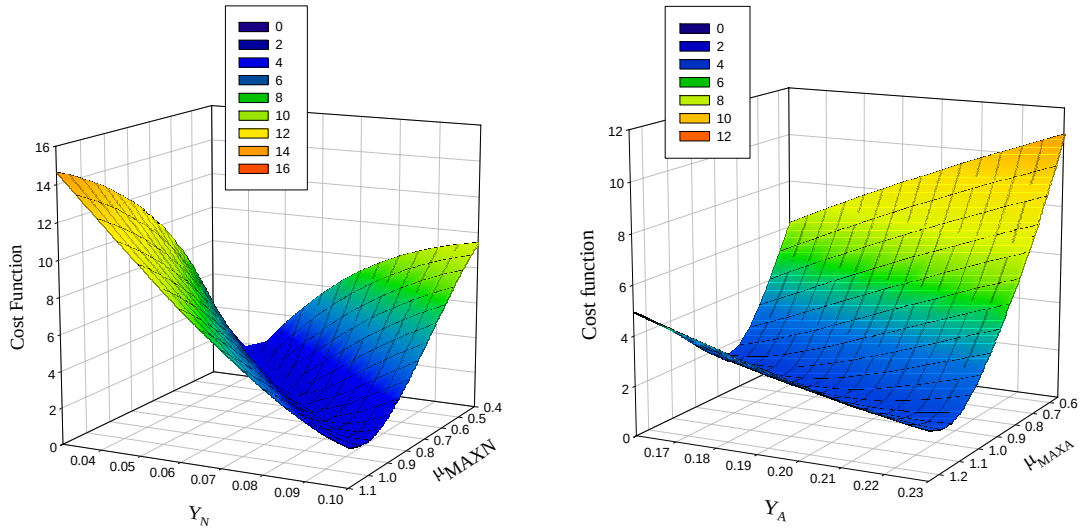

Figure VI.B3 Sensitivity functions for μ_A and Y_N (LEFT) μ_N and Y_A (RIGHT) experiment with two pulses addition of 18.75 mg N-NH_4^+/L and 18.75 mg NO_2^-/L

Afterwards, Petersen conducted a practical identifiability study on the same model and surprisingly, the FIM obtained became singular indicating an unidentifiable scenario. Hence, the results obtained using the FIM as a measure for local parameter identifiability differed to the theoretical identifiability studies. The reasons for this discrepancy were not clear and Petersen hypothesised on information lost when linearising the model. To avoid any identifiability inconsistency, both Y_A and Y_N were previously calculated together.

The biomass growth yield could theoretically be assessed with the initial substrate value and the total oxygen consumed. Hence, only one batch experiment would be required. However, a sole experiment results in too much uncertainty on yield calculation since small deviations in the total oxygen consumption imply high variations in the yield value. Table VI.B2 shows the variance in the estimated yield value for NOB with small variations on the total oxygen consumed (see equation VI.B14 above). A 5% error in the total oxygen consumed estimation is amplified up to 40 % in the Y_N estimation.

Table VI.B2 Simulation of Y_N estimation error as a function of the total oxygen consumption error in one sole nitrite pulse

Initial $N\text{-}NO_2^-$ load (mg N)	Simulated oxygen consumed (OC) ($mg\ O_2$)	Y_N ($1.14\text{-}OC/N\text{-}NO_2^-$) ($g\ COD_X/g\ N$)
10.0	9.50	0.19
10.0	9.75	0.17
10.0	10	0.14
10.0	10.25	0.12
10.0	10.5	0.09

To overcome this problem, the total oxygen consumed in several pulses with different loads of $N\text{-}NH_4^+$ and $N\text{-}NO_2^-$ was measured (experiments VI.B1 and VI.B2, respectively). These experiments were performed using ammonium chloride as AOB substrate and sodium nitrite as NOB substrate in this load range: 5-10-15-20-30 mg N/L. The total oxygen consumption (as the area under the OUR profile) was estimated for each pulse.

Table VI.B3 Experiment VI.B1

EXPERIMENT VI.B1	Y_N estimation
Equipment	LFS respirometer (V_0 = 0.8 L)
pH	7.5
Temperature	25 ºC
Acid used	HCl = 0.25 M
Base used	NaOH = 0.25 M
Pulses	5-10-15-20 mg $N\text{-}NO_2^-$

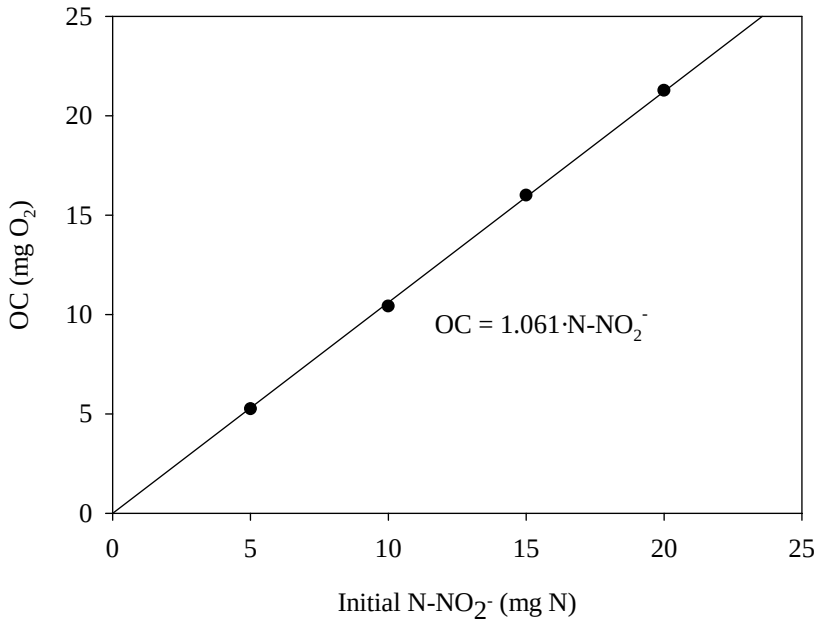

Figure VI.B4 Total oxygen consumed in a pulse of $N\text{-}NO_2^-$ versus the nitrogen (as nitrite) load

The slope of the regression line obtained when plotting the oxygen consumed versus the total $N\text{-}NO_2^-$ added was 1.06 g O_2/g N. If ammonium traces were assumed to be the nitrogen source for NOB (Wallace and Nicholas, 1968; Gapes *et al.*, 2003), then the entire $N\text{-}NO_2^-$ added would be oxidised to $N\text{-}NO_3^-$. The NOB yield could be estimated through equation VI.B14 (according to the two-step model described in Table VI.A3).

$$1.06 = \frac{-\left(\frac{1.14}{Y_N} - 1\right)}{\frac{1}{Y_N}} \qquad \text{(VI.B14)}$$

where Y_N = 0.08 g COD_X/g N

In any case, if nitrite was considered as the nitrogen source, Y_N would be calculated with expression VI.B15 and practically the same value of Y_N would be obtained.

$$1.06 = \frac{-\left(1.14\left(\frac{1}{Y_N} + i_{NB}\right) - 1\right)}{-\left(\frac{1}{Y_N} + i_{NB}\right)} \qquad \text{(VI.B15)}$$

Experiment VI.B2 was conducted for Y_A estimation which was somehow more complex, since part of the $N\text{-}NH_4^+$ was directly incorporated into biomass for growth instead of being oxidised.

Table VI.B4 Experiment VI.B2

EXPERIMENT VI.B2	Y_A estimation
Equipment	LFS respirometer (V_0 = 0.8 L)
pH	7.5
Temperature	25 ºC
Acid used	HCl = 0.25 M
Base used	NaOH = 0.25 M
Pulses	5-10-15-30 mg $N\text{-}NH_4^+$

Chandran and Smets (2001) already pointed out that ignoring this fact may induce to a huge error of yield overestimation. According to the model stoichiometry shown on Table VI.A3, the total oxygen consumed for an ammonium pulse could be calculated with expression VI.B16. This expression sums up the total oxygen required to oxidise the ammonium not incorporated to the biomass to nitrite and afterwards the nitrite to nitrate.

Figure VI.B5 shows the total oxygen consumed as a function of the initial ammonium load and the regression line used for Y_A estimation. The slope of the regression line was 4.22.

$$4.22 = \frac{-\left(\frac{3.43}{Y_A} - 1\right)}{-\left(\frac{1}{Y_A} + i_{NB}\right)} + \frac{\frac{1}{Y_a}}{\left(\frac{1}{Y_A} + i_{NB}\right)} \cdot \frac{-\left(\frac{1.14}{Y_A} - 1\right)}{-\frac{1}{Y_A}} \qquad \text{(VI.B16)}$$

Hence, Y_A= 0.21 g COD_X/g N

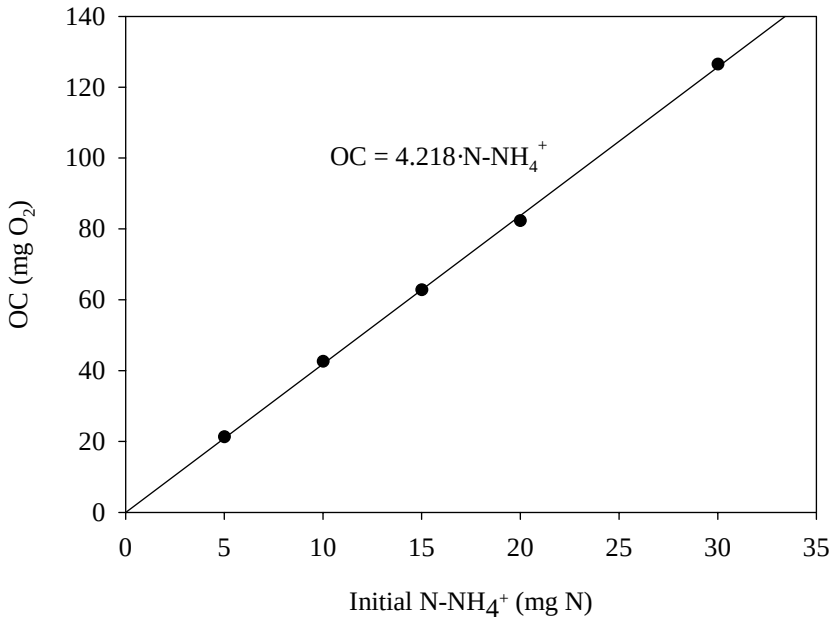

Figure VI.B5 Total oxygen consumed in a pulse of $N\text{-}NH_4^+$ versus the initial nitrogen load

As explained before, a common error in the literature is to estimate Y_A without considering the amount of nitrogen incorporated into the biomass (Chandran and Smets, 2001). In these cases, the yield is erroneously calculated using expression VI.B17 and the value obtained (Y_A=0.273) overestimates the real yield value in 24%. This error would influence a lot in the estimation of the model parameters, particularly of those which are somehow correlated with the yield, such as the growth rate.

$$4.218 = \frac{-\left(\frac{4.57}{Y_A + Y_N} - 1\right)}{-\frac{1}{Y_A + Y_N}} \qquad \text{(VI.B17)}$$

Table VI.B3 compares the results obtained in this work with other yields found in the literature. As can be observed, there exists a wide range of values and it is difficult to know whether this range truly exists (i.e. the nitrifying biomass has a highly variable yield) or there are a lot of erroneous works (i.e. correlations in parameter estimation not taken into account). The last column in the table shows that it is widely accepted that the Y_A is always 2-3 times higher than Y_N.

Table VI.B3 Comparison of the obtained yields with the literature

Reference	Y_A (g COD_X/ g $N\text{-}NH_4^+$)	Y_N (g COD_X/ g $N\text{-}NO_2^-$)	Y_A/Y_N
This work	0.21	0.08	2.62
Wiessmann (1994)	0.147	0.042	3.5
Knowles *et al.*, (1965)	0.05	0.02	2.5
Sheintuch *et al.*, (1995)	0.14	-	
Gee *et al.*, (1990a)	0.43[1]	0.132[1]	3.25
Gee *et al.*, (1990b)	0.40[1]	0.114[1]	3.5
Copp and Murphy (1995)		0.015	
Hellinga *et al.,*(1999)	0.15	0.041	3.65
Gapes *et al.,* (2003)	0.082	0.04	2.05
EPA (1993)	0.057-0.185[1,2]	0.028-0.099[1,2]	2

[1] the original parameters were in g VSS/g N units and they were transformed in g COD_X/ g N using 1.42 g COD_X/g VSS

[2] calculated for pure cultures of *Nitrobacter* and *Nitrosomonas*

VI.B.3.4 GROWTH AND DECAY PARAMETERS: μ_A, μ_N, f_A, f_N, b_A, b_N and f_{XI}

$\mu_{MAX,A}$: AOB maximum growth rate (1/d)
$\mu_{MAX,N}$: NOB maximum growth rate (1/d)
f_A : AOB active fraction
f_N : NOB active fraction
b_A : AOB decay rate constant (1/d)
b_N : NOB decay rate constant (1/d)
f_{XI} : inert fraction on lysis products

Active fraction is a very particular parameter since its existence is known but few authors mention it and even less try to estimate it. As the complexity of models increase, the number of biomass fractions (heterotrophs, nitrifying, denitrifying, PAOs, DPAOs,…) and the number of internal storage polymers considered (PHAs, glycogen, polyphosphate…) also increase. With just a VSS measurement, which includes all these compounds, the model cannot be calibrated. The rates of the different processes are directly linked to the active fractions of the biomass, however these parameters cannot be measured directly and this introduces an important doubt in the reliability of the models developed nowadays.

In short-term batch low-loaded experiments, where growth and decay are practically negligible, the value of active fraction is totally correlated to the value of the maximum growth rate and the decay rate. Figure VI.B6 shows the existing severe correlation between growth rate and active fraction. This correlation is even more important if it is observed that this plot has been developed in a wide range of μ and f values. Hence, the values of μ and f cannot be estimated in a reliable way separately using OUR and HPR. The parameter combinations $\mu_A \cdot f_A$ and $\mu_N \cdot f_N$ are estimated and, afterwards, f_A and f_N (and μ_A and μ_N) are approximated using the endogenuous OUR value.

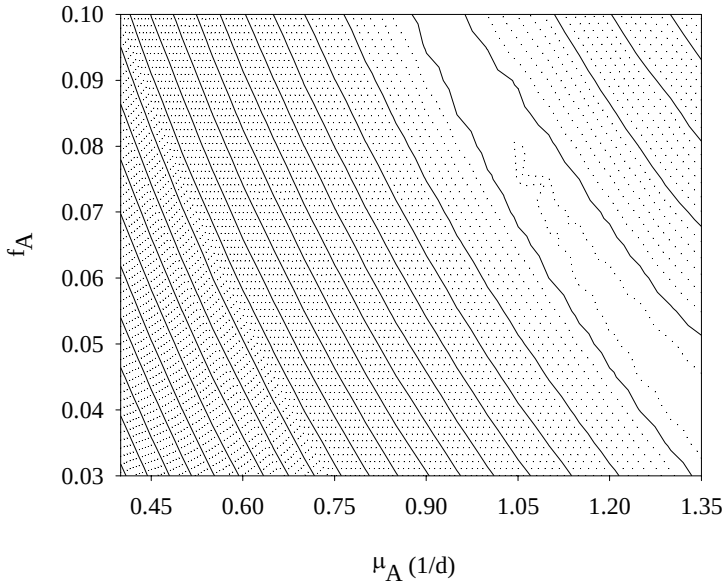

Figure VI.B6 Contour plot of the cost function with small f_A and μ_A variations for an ammonium pulse

Some experiments have been proposed to estimate the active fraction based on the biomass decay and as such these are long experiments. Ubisi *et al.* (1997) measured the OUR of heterotrophic population a day after a pulse of substrate was added to estimate the heterotrophic active fraction. Jubany *et al.* (2004) proposed an efficient alternative

using three different substrate pulses in a period of approximately 30 hours, where the active fraction is calculated taking into account the growth and the decay of biomass.

Nevertheless, the active fraction values can be roughly approximated using the endogenous OUR value according to the two-step model previously described (Table VI.A3). The endogenous OUR value corresponded to the next expression:

$$OUR_{END} = (1 - f_{XI}) \cdot b_A \cdot X_A + (1 - f_{XI}) \cdot b_N \cdot X_N \quad \text{(VI.B18)}$$

If X_i was considered $f_i \cdot X$ (no net change in X was considered in low-loaded and short-term batch experiments), the expression obtained was:

$$OUR_{END} = (1 - f_I) \cdot b_A \cdot X \cdot f_A + (1 - f_I) \cdot b_N \cdot X \cdot f_N \quad \text{(VI.B19)}$$

Once the OUR_{END} value was known, there were five unknown variables. Experimental f_{XI} determination was quite tedious. Moreover, it was a parameter with very low sensibility on short-term output measurements, hence it could be assumed from the literature (ASM2 default value was f_{XI}=0.2). The decay rates for AOB or NOB are generally considered equal. Jubany *et al.* (2004) estimated the value of b_N for NOB used in this experiments at b_N= 0.14 1/d. This value was in agreement with the default value proposed by ASM2 (0.15 1/d) and was assumed for both populations. After assuming f_{XI} and calculating both b_I, there were still two unknown parameters (f_A and f_N) and one equation. An extra equation was needed, which derived from the assumption that the ratio between fractions (f_A/f_N) is equal to the ratio between yields (Y_A/Y_N) (Gee *et al.*, 1990a).

Hence, μ_A and μ_N can be approximated with only the value of OUR_{END} and the parameter estimation results. A practical utilisation of this procedure with experimental values can be seen in Section VI.E.2.

VI.B.4 INITIAL VALUES

As the model involves ordinary differential equations, the initial values of the state variables are required for model simulation. Most of these values are calculated according to the pulse additions:

$S_{NH3}(0)$ (initial nitrogen in form of ammonia) and **$S_{NH4}(0)$** (initial nitrogen in form of ammonium) are calculated using the initial amount of ammonium-nitrogen added: (NT) [eq. VI.B20a,b].

$$S_{NH4}(0) = \frac{NT}{1 + 10^{pH - pK3}}$$
$$S_{NH3}(0) = \frac{NT}{1 + 10^{pK3 - pH}} \quad \text{(VI.B20a,b)}$$

$S_{HNO2}(0)$ (initial nitrogen in form of nitrous) and **$S_{NO2}(0)$** (initial nitrogen in form of nitrite) are calculated using the initial amount of nitrite-nitrogen added: (NOT) [eq. VI.B21a,b].

$$S_{HNO2}(0) = \frac{NOT}{1 + 10^{pH - pK4}}$$
$$S_{NO2}(0) = \frac{NOT}{1 + 10^{pK4 - pH}} \quad \text{(VI.B21a,b)}$$

$S_{CO2}(0)$ (initial carbon dioxide) and **$S_{HCO3}(0)$** (initial bicarbonate) are calculated from the total inorganic carbon (TIC) in the system through equations VI.B22 a and b. This value must estimated using the model, because the initial amount of TIC in the reactor before the pulse addition is difficult to measure. Therefore, the estimated value should be higher than the amount of bicarbonate added.

$$S_{CO2}(0) = \frac{TIC}{1 + 10^{pH-pK1}}$$
$$S_{HCO3}(0) = \frac{TIC}{1 + 10^{pK1-pH}} \qquad \text{(VI.B22a,b)}$$

$S_{NO3}(0)$ (initial nitrogen in form of nitrate), **$S_{HP}(0)$** (initial proton concentration) and **$X_I(0)$** (initial inert concentration) are set to zero and **$S_{O2}(0)$** (initial dissolved oxygen) is measured.

$X_A(0)$ (initial AOB concentration) and **$X_N(0)$** (initial NOB concentration) are estimated through the initial biomass fractions [eq VI.B23a,b].

$$X_{A(0)} = X_{(0)} \cdot f_A \qquad \text{(VI.B23a)}$$
$$X_{N(0)} = X_{(0)} \cdot f_N \qquad \text{(VI.B23b)}$$

Chapter VI.B Conclusions

- The physical-chemical parameters for the two-step nitrification model (except for the k_La_{O2}, k_La_{CO2} and pK_1) can be obtained from the literature and maintained constant as long as the operational conditions coincided with the conditions under which these parameters were estimated.
- The biomass composition obtained in this thesis was $C_{0.2}H_{1.54}O_{0.4}N_{0.18}$, which corresponded to a i_{NB} = 0.075 g N /g COD_X.
- According to the parameter identifiability, an experiment to estimate both yields would be very helpful for parameter estimation reliability.
- The biomass growth yields for both populations should be calculated taking into account that part of the ammonia is directly incorporated in the biomass. For the populations used in this thesis, the yields were:
  - Y_A = 0.207 g COD_X/g N and Y_N = 0.080 g COD_X/g N
- Active fraction is a very particular parameter since its existence is known but few authors mention it and even less try to estimate it. The active fraction values can be roughly approximated using the endogenous OUR value according to the two-step model previously described.

CHAPTER VI.C

Respirometric estimation of the oxygen affinity constants for biological ammonium and nitrite oxidation

This chapter has been published as:

Guisasola A., Jubany I., Baeza J.A., Carrera J. and Lafuente J. (2005b). Respirometric estimation of the oxygen affinity constants for biological ammonium and nitrite oxidation. J. Chem. Technol. Biotechnol. 80(4), 388-39.

ABSTRACT

The aim of this chapter is to qualitatively and quantitatively assess the limitation effect of DO and inorganic carbon on nitrifying biomass. The nitrification process is a two step process with nitrite as an intermediate product. As it is an aerobic process, its kinetics is highly dependent on the DO concentration in the medium. This limitation is generally described using Monod-type kinetics with K_O as the oxygen affinity constant. Many authors do not estimate the values of the K_{OA} and K_{ON} (affinity constants for nitritation and nitratation, respectively) but assume them from the literature. This assumption may be acceptable when working at high DO levels. However, these values have recently gained a lot of importance, particularly in view of modelling tasks, since new alternatives to the classical BNR at low DO values have appeared. A critical review of different K_O estimation methods is developed and a new procedure which improves previous methodologies is proposed. This new procedure considers the oxygen surface transfer and the DO probe time response. The results obtained were K_{OA} = 0.74 ± 0.02 mg O_2/L and K_{ON} = 1.75 ± 0.01 mg O_2/L.

VI.C.1 Impact of oxygen limitations on nitrification

As oxygen supply represents a very important cost in most of the wastewater treatment plants (WWTP), the DO concentration is usually maintained at a low level (around 2 mg O_2/L). Hence, aerobic activated sludge processes such as COD removal, nitrification and aerobic P–uptake may be occurring under oxygen limitations. The oxygen limitation is known to have more influence on nitrification than on the heterotrophic processes since both K_O values for nitrification are described to be higher than the ones proposed for heterotrophic processes. Then, researchers need to evaluate how this oxygen limitation would affect to the process rate.

In the nitrification case, the total oxygen required in the whole nitrification process is 4.57 g O_2/g N-NH_4^+ oxidised. The first step requires 3.43 g O_2/g N-NH_4^+ and the second step 1.14 g O_2/g N-NO_2^-. The nitrification kinetics dependence on the DO concentration is generally described using the Monod expression [eq. VI.C1]. As can be deduced, the K_O represents the DO concentration at which the nitritation or nitratation rate becomes half of the maximum nitritation or nitratation rate.

$$r = r_{max} \cdot \frac{S_O}{K_O + S_O} \qquad \text{(VI.C1)}$$

where,

r = nitritation or nitratation rate (mg N/mg VSS/d)
r_{max} = maximum nitritation or nitratation rate (mg N/mg VSS/d)
S_O = dissolved oxygen concentration (mg O_2/L)
K_O = AOB or NOB affinity constant for DO (mg O_2/L)

Many authors do not estimate the values of the K_{OA} and K_{ON} (affinity constants for nitritation and nitratation, respectively) but assume them from the literature. This assumption may be acceptable when working at high DO levels. However, these values have recently gained a lot of importance, particularly in view of modelling tasks, since new alternatives to the classical BNR at low DO values have appeared. These technologies aim at a partial inhibition of the nitratation by favouring the nitritation step is favoured and accumulating nitrite. This technology (i.e. partial nitrification or nitrification via nitrite) could suppose a 25 % reduction of the total oxygen requirements as well as a reduction in the amount of sludge produced.

Several strategies have been tested to achieve partial nitrification. The main difference among them is how to favour the nitritation step in front of the nitratation. Many authors have accumulated nitrite based on the lower NOB affinity for the DO compared to AOB

(Garrido *et al.*, 1997; Kuai and Verstraete, 1998; Bernet *et al.*, 2001, Bae *et al.*, 2002; Pollice *et al.*, 2002; Ruiz *et al.*, 2003; Wyffels *et al.*, 2003; Jianlong *et al.*, 2004). Laanbroek and Gerards (1993) studied the competition for oxygen using pure cultures (*Nitrosomonas europaea* and *Nitrobacter winogradski*). They found that ammonia oxidisers have a higher affinity for oxygen than nitrite oxidisers. Thus, partial nitrification can be achieved by choosing a certain DO set-point where the nitritation rate is not as much oxygen limited as the nitratation rate.

Another possible methodology is the SHARON® process, which makes use of the different growth rates of AOB and NOB at high temperatures (30-35 ºC) by working at a hydraulic retention time (HRT) higher than the growth rate of NOB but lower than AOB (about 1 day) and without sludge retention (e.g. Hellinga *et al.*, 1998; Hellinga *et al.*, 1999 or Schmidt *et al.*, 2003 among others). Finally, the fact that NOB is more inhibited by free ammonia (FA) than the AOB has also been described in the literature as a procedure for partial nitrification (Anthonisen *et al.*, 1976).

As the first strategy (DO limitation) is gaining importance, reliable values for the oxygen affinity constants of both processes are required to correctly model this new methodology. Moreover, knowing the values of both K_O constants can help the WWTP manager to choose a proper DO set-point in periods when nitrification is decaying (e.g. in winter season due to low temperatures).

VI.C.2 K_O estimation methodology

VI.C.2.1 CONCEPTUAL DESCRIPTION

The oxygen affinity constant for a certain process can be generally estimated in two different ways (likewise all the Monod affinity constants):

a) measuring the maximum process rate at different oxygen setpoints (Sanchez *et al.* 2001; Weon *et al.*, 2004).

b) monitoring the process rate decrease when external aeration is stopped and the DO concentration falls down. This second procedure was successfully applied by Wiesmann (1994) for K_{ON} estimation and an extension of this technique was employed in this chapter to estimate both K_{OA} and K_{ON}. The main modifications included, apart from a different mathematical approach to the problem, were the contemplation of the oxygen transfer from the atmosphere, the response time of the DO probe and the inhibition of the nitratation step with sodium azide when estimating K_{OA}.

The procedure developed in this work consisted of monitoring the DO drop in the respirometric vessel when the aeration was turned off and the biomass was consuming without substrate (ammonium or nitrite) limitations. The sludge used in this work was a biomass particularly enriched in nitrifying microorganisms because it was grown in a pilot plant fed with a very low COD/N ratio (see Chapter III.1.6).

A pulse of substrate was added to the respirometer and, once the maximum rate was reached, the aeration was stopped. At this moment, the DO in the liquid phase sharply decreased because of the oxygen consumption linked to the substrate consumption. This oxygen consumption rate corresponded to the maximum OUR assuming that no substrate (ammonium or nitrite) limitations existed. It was essential to avoid any substrate limitation (except from oxygen) for a reliable K_O estimation. The nitritation or nitratation rate decreased as the DO concentration also decreased in the respirometer because of oxygen limitations. The lower the DO level was, the more important the oxygen limitation effect.

The system without neither external aeration nor substrate limitations should be described with equation VI.C2

$$\frac{dSo}{dt} = -OUR_{END} - OUR_{MAX} \quad \text{(VI.C2)}$$

Nevertheless, this expression is not valid in most of the experimental setups used, because apart from the oxygen limitation effect, the oxygen transfer through the liquid-gas surface needs to be considered. This transfer is generally despised in front of the oxygen transfer due to the system external aeration. However, in some open and stirred systems without external aeration, this transfer may acquire enough importance to be considered. Although the liquid-gas surface area was minimised as much as possible during the experiments, it will be demonstrated below that this transfer should not be ignored. During the DO drop, the DO reached levels close to zero, which imply high levels of driving force for oxygen transfer through the liquid-gas surface: $[S_O^*-S_O(t)]$. Thus, the expression that better describes the system is equation VI.C3:

$$\frac{dSo}{dt} = k_L a^{SYP} \cdot [S_O^* - S_O(t)] - (OUR_{END} + OUR_{MAX}) \frac{S_O}{K_O + S_O} \quad \text{(VI.C3)}$$

where k_La^{SUP} is the global oxygen transfer constant through the liquid-gas surface and OUR_{MAX} is defined as a function of the substrate used (equations VI.C4a,b)

$$OUR_{MAX} = \frac{3.43 - Y_A}{Y_A} \cdot \mu_{MAXA} \cdot X_A \text{ for AOB} \quad \text{(VI.C4a)}$$

$$OUR_{MAX} = \frac{1.14 - Y_N}{Y_N} \cdot \mu_{MAXN} \cdot X_N \text{ for NOB} \quad \text{(VI.C4b)}$$

VI.C.2.2 k_La^{SUP} ASSESSMENT

As aforementioned, the oxygen transfer through the liquid-gas surface must be taken into account (note that the system was continuously stirred). This transfer depends on the volumetric oxygen mass transfer constant (k_La^{SUP}), which derives from a multiplication of k_L (surface oxygen transfer constant) and *a* (ratio between surface area and volume of the reactor). In this work, k_L was estimated in a previous experiment VI.C1 where the endogenous OUR (OUR_{END}) was measured at different values of *a*. This OUR value was calculated as the slope of the DO decrease in the reactor without external aeration and without external substrate. Due to the liquid-gas surface oxygen transfer, this value was not the exact OUR_{END} but an apparent endogenous OUR (OUR^{APP}_{END}) which included both effects. The experimental profiles obtained are plotted on Figure VI.C1. This experiment was conducted under the same operational conditions (pH, T and stirring) as in the further K_O estimation experiments, except for the vessel which was an Erlenmeyer (500 mL) to obtain a wide range of values of *a*.

As can be seen in Figure VI.C1, the lower the parameter *a*, the higher the OUR^{APP}_{END} value. This is understandable since a decrease in the contact area implies less oxygen transferred from the atmosphere and the "subestimation" error on the OUR_{END} measurement is lower. Hence, the intercept value of the regression (the OUR^{APP}_{END} for *a*=0) can be considered as the "real" endogenous value (i.e. without surface oxygen transfer). Then, OUR^{APP}_{END} can be described as a function of the parameter *a*, according to equation VI.C5:

$$OUR^{APP}_{END}(a) = OUR_{END} - k_L a^{SUP} \cdot (S_O^* - S_O) \quad \text{(VI.C5)}$$

where k_L can be calculated from the slope of the regression above [eq. VI.C6]:

$$k_L = \frac{slope}{(S_O^* - S_O)} \qquad \text{(VI.C6)}$$

OUR^{APP}_{END} values for each "*a*" were calculated between the same limits of DO (from 6.6 to 6 mg O_2/L approximately). Hence, the mean S_O in the decrease was 6.3 mg O_2/L. S_O^* is 8.49 mg O_2/L at 25 ºC. If the driving force (S_O^*- S_O) was assumed to be 2.2 (obtained from 8.5 - 6.3), the value of k_L calculated would be 8.33 $m^3/m^2/d$. Finally, as the measured parameter "*a*" in the respirometric vessel employed in this work was 0.49 m^2/m^3, the value of the k_La^{SUP} estimated was 4.08 1/d. This value will be used below for K_O estimation.

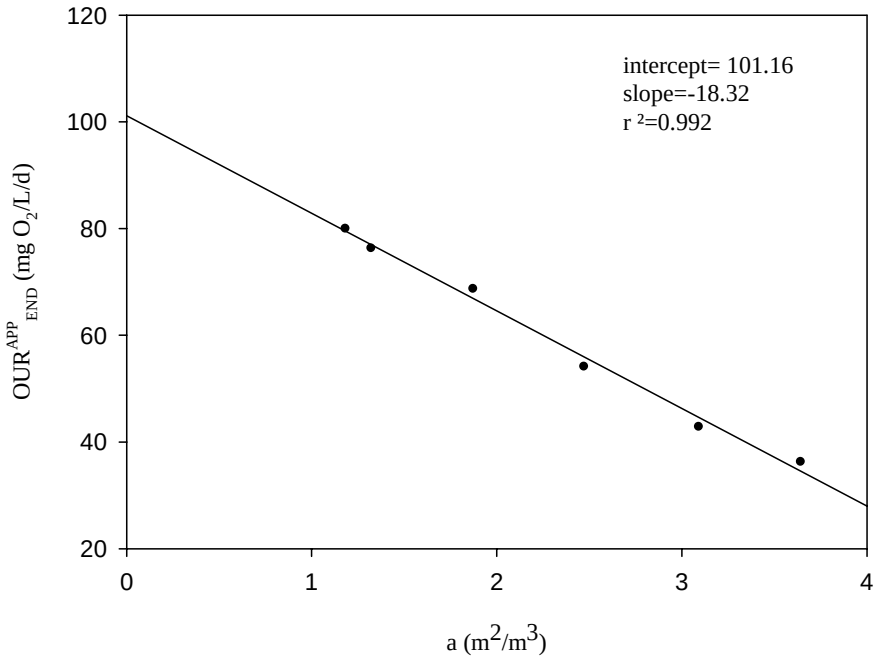

Figure VI.C1 Dependence of the OUR^{APP}_{END} on the parameter *a*

VI.C.2.3 DO PROBE TIME RESPONSE

The time response of the DO probe is not a negligible parameter, particularly in fast experiments with sharp/sudden DO changes. The importance of this parameter arises in low data collection frequency experiments. In this thesis, the time constant for the DO probe was calculated for a proper K_O estimation, especially for the K_{OA} where the experiments performed accomplish the conditions aforementioned.

The DO probe time constant was estimated using positive and negative steps to the measured output (DO concentration). These steps were achieved with two different samples of water bubbled with air and nitrogen respectively (Figure VI.C2). For instance, the negative step was obtained with an instantaneous change of the DO probe submerged in the air-bubbled water to the nitrogen-bubbled water. Assuming that the DO probe behaved as a first order system (Stephanopoulos, 1984), the DO profile obtained with this immediate change could be fitted to the next expression:

$$S_O(t) = S_O^{INITIAL} + K \cdot (1 - e^{-t/\tau}) \qquad \text{(VI.C7)}$$

where,

K = absolute value of the step (mg O_2/L)
τ = DO probe time constant (s)
$S_O^{INITIAL}$ = S_O concentration at t=0 (mg O_2/L)

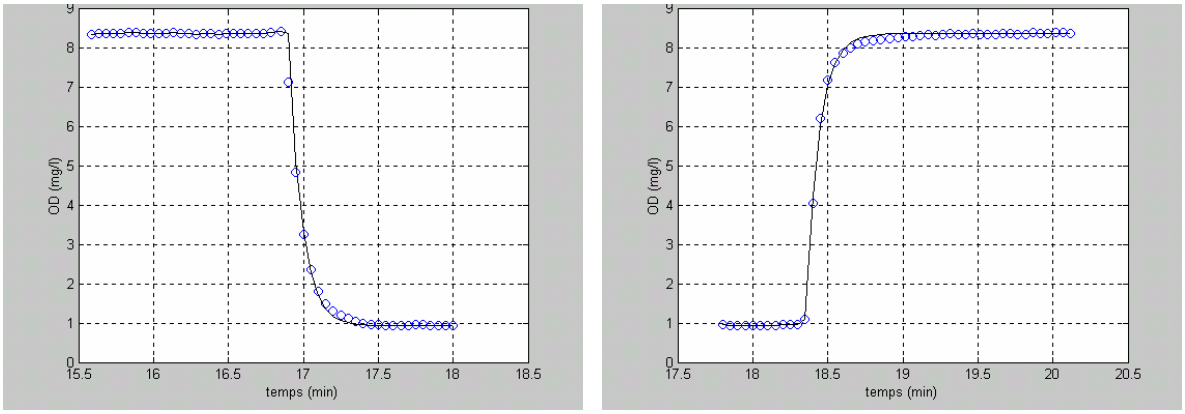

Figure VI.C2 DO probe time constant assessment

In this work, the DO probe time constant was calculated to be 5.8 seconds. Then, the measured DO values should be corrected according to the next expression:

$$S_O^{CORR}(t) = \frac{S_O^{MEAS}(t) - (1-\alpha)\cdot S_O^{MEAS}(t-1)}{\alpha} \qquad \text{(VI.C8)}$$

where,

S_O^{CORR} = corrected DO concentration (mg O_2/L)
S_O^{MEAS} = measured DO concentration (mg O_2/L)
$\alpha = \Delta t / (\Delta t + \tau)$ and Δt = data collection frequency

VI.C.2.4 NITRATATION INHIBITION WITH SODIUM AZIDE

Nitratation inhibition is required for the correct calculation of K_{OA}. Otherwise, the measured OUR will correspond to the sum of the OUR due to ammonium oxidation and the OUR linked to the nitrite consumption produced during the nitritation step. Only the OUR related to the ammonium consumption should be used when estimating K_{OA}. The nitratation step was inhibited using sodium azide as described before (Ginestet *et al.*, 1998). Nevertheless, experiment VI.C2 (Table VI.C1) was performed to ensure that the experimental concentration of sodium azide added only inhibited nitratation and had minimal effect upon nitritation.

Table VI.C1 Experiment VI.C2

EXPERIMENT VI.C2	Inhibition of nitratation with sodium azide
Equipment	LFS respirometer (V_0 = 1 L)
pH	7.5
Temperature	25 ºC
Acid used	HCl = 0.25 M
Base used	NaOH = 0.25 M
Pulses	25 mg N-NH_4^+ (t=70 min)
	24 μmol sodium azide
	25 mg N-NH_4^+
	25 mg N-NO_2^-

According to Figure VI.C3, when a pulse of 25 mg/L of nitrogen as ammonium was added without inhibitor (first pulse), it was possible to differentiate the two steps of the nitrification process. The nitratation step was slower than the nitritation step under the experimental conditions used in this thesis. The total oxygen consumption related to this pulse (corresponding to the area under the OUR profile) was 108.4 mg O_2. This indicated a global biomass yield for the nitrification of 0.23 g COD_X/g N, which was in the range of the reported values in the literature (Table VI.B3)

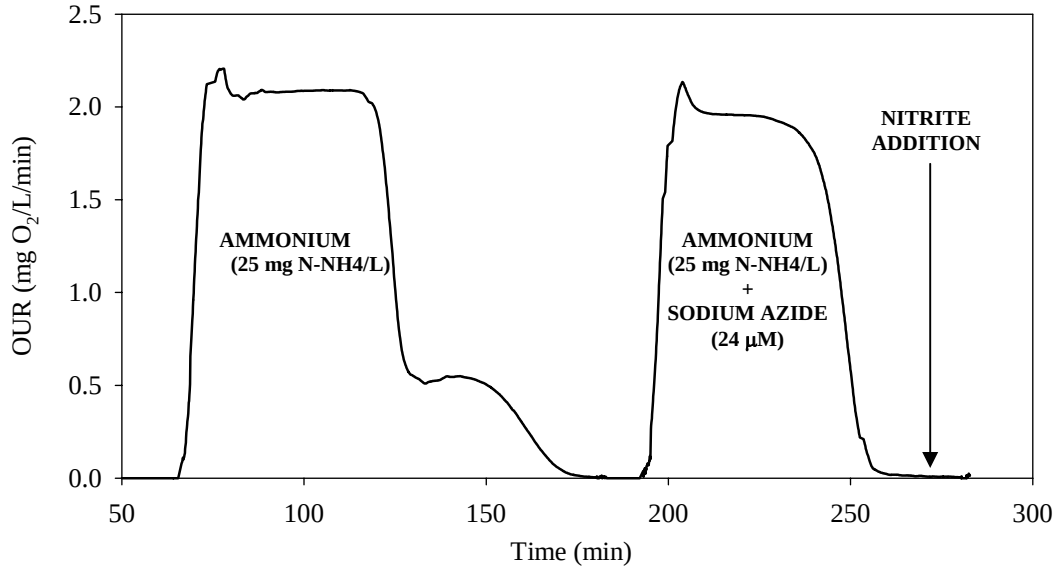

Figure VI.C3 Assessment of nitratation inhibition using sodium azide (24 μM)

The second pulse corresponded to the simultaneous addition of ammonium (25 mg N-NH_4^+/L) and sodium azide (24 μM). At first glance, the second shoulder corresponding to the nitratation step was not observed, which would clearly indicate the inhibition occurrence. Moreover, the oxygen consumed in this second pulse was 81.75 mg O_2. The ratio of this value on the oxygen consumed in the pulse without inhibition was 0.754 which was in agreement with the stoichiometric ratio: 0.750 (= 3.43 / 4.57). This value illustrated that the nitritation step is not inhibited at all with the amount of sodium azide added. Finally, a third pulse of nitrite was added to confirm the nitratation inhibition and no response in terms of oxygen consumption was observed.

VI.C.3 K_{OA} and K_{ON} estimation results

Experiments VI.C3 and VI.C4 were conducted for K_{ON} and K_{OA} estimation. Each experiment consisted in two DO drops to estimate the K_O value. Once the pulse of substrate was added, the aeration was turned off and the DO drop was monitored in the respirometric. The experimental DO profiles obtained without neither external aeration nor substrate limitations are depicted in Figures VI.C4 (AOB biomass) and VI.C5 (NOB biomass). In experiment VI.C3, the nitratation step was inhibited with sodium azide (24 μM) These experimental DO drops could be described using the ordinary differential equation VI.C3.

Table VI.C2 Experiment VI.C3

EXPERIMENT VI.C3	K_{OA} estimation
Equipment	LFS respirometer (V_0 = 0.8 L)
pH	7.5
Temperature	25 ºC
Acid used	HCl = 0.25 M
Base used	NaOH = 0.25 M
Pulses	25 mg N-NH_4 (t = 0)
	24 μmol sodium azide (before pulse)

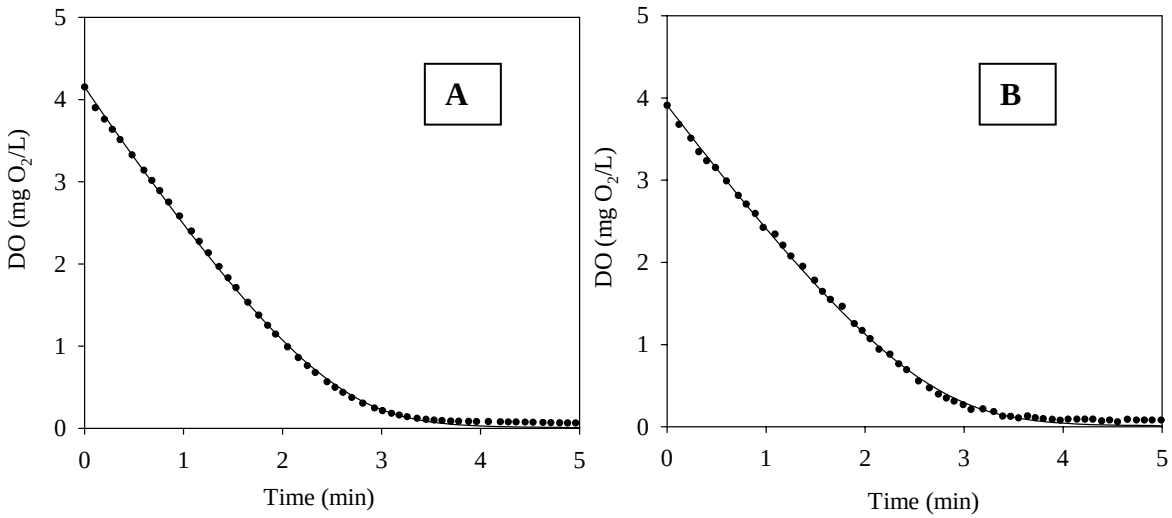

Figure VI.C4 (A, B) Experimental DO decrease for ammonium as substrate : experimental data (dotted line) and modelled data (solid line)

Table VI.C3 Experiment VI.C4

EXPERIMENT VI.C4	K_{ON} estimation
Equipment	LFS respirometer (V_0 = 0.8 L)
pH	7.5
Temperature	25 ºC
Acid used	HCl = 0.25 M
Base used	NaOH = 0.25 M
Pulses	25 mg N-NO_2 (t=0)

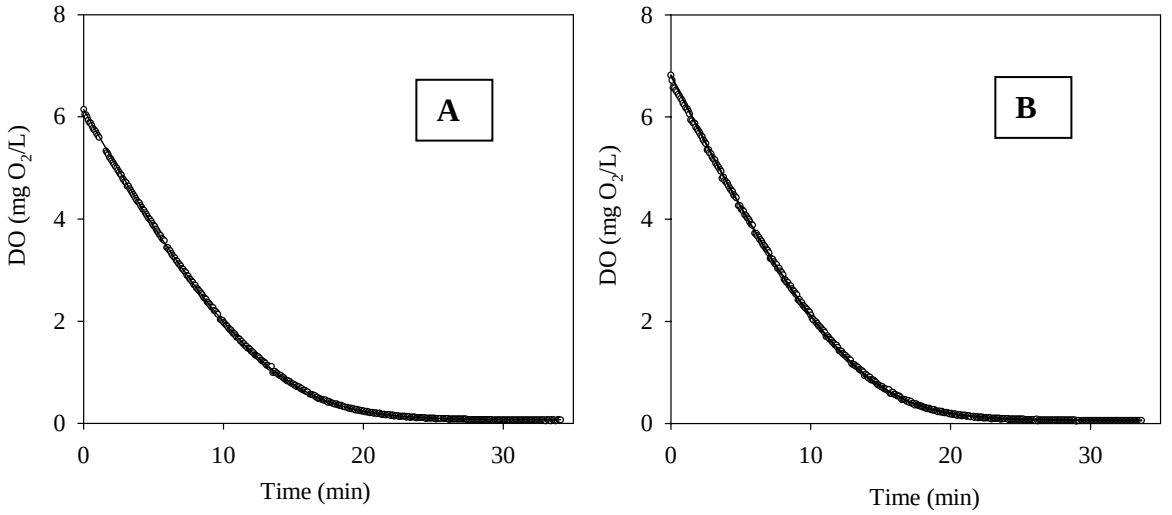

Figure VI.C5 (A, B) Experimental DO decrease for nitrite as substrate: experimental data (dotted line) and modelled data (solid line)

K_{OA} and K_{ON} were estimated by fitting the experimental DO profiles to equation VI.C3. K_O estimation results obtained as an average of both experiments (A,B) for each of the processes are : K_{OA} = 0.74 ± 0.02 mg O_2/L and K_{ON} = 1.75 ± 0.01 mg O_2/L. The parameters were estimated for a confidence level of 95 %. The parameter estimation error predicted for K_{OA} using the FIM methodology was twice the one predicted for K_{ON}. This was understandable since the experiments with nitrite as substrate were slower and, then, the data collection and the information amount increased. However, in both cases, the parameter estimation errors were very small, so the estimated K_O values could be considered quite reliable.

Table VI.C5 compares the estimated K_O values with different K_O values found in the literature. As can be seen the values estimated in this study were considerably higher than the default ones used in the classical Activated Sludge Model nº1 (Henze *et al.*, 2000). This fact would cause an important error when estimating the values of μ_{MAX} and K_S from respirometric batch experiments using 0.4 as the K_O value if the working DO level was lower than 3 mg O_2/L.

Table VI.C5 K_O values obtained in this study and from the literature

Affinity constant for DO (mg O_2/L)			
AOB (K_{OA})	NOB (K_{ON})	Temperature (ºC)	Reference
0.74 ± 0.02	1.75 ± 0.01	25	This study
1.45	1.1	35	Hellinga et al. (1998)
1.66*	3*	30	Sánchez et al. (2001)
0.6	1.3	20	Weissmann (1994)
0.5-2		25	EPA (1993)
0.4		25	Henze et al. (2000)
0.16	0.54	30	Hunik et al. (1994)
0.3	0.6	28	Nowak et al. (1995)
From 0.27 to 1.61	0.87 to 1.1	From 30ºC to 5ºC	Weon et al. (2004)

*Obtained at 24 g NaCl/L

Weon *et al.* (2004) studied the dependence of these oxygen constants with temperature and observed an inverse proportion. However, the degree of proportion was different for each constant and K_{OA} seemed strongly affected by the temperature. This strong dependence resulted in the fact that at temperatures lower than 17 ºC the K_{OA} was higher than K_{ON} and for temperatures higher than 17ºC K_{ON} was higher than K_{OA}, which was in agreement with the results found in this thesis.

K_O values neglecting surface oxygen transfer were estimated to confirm that this transfer should be taken into account. The K_{OA} obtained was 0.75 ± 0.02 mg O_2/L and the K_{ON} was 2.320 ± 0.015 mg O_2/L. As expected, neglecting oxygen transfer implied an overestimation of the constants, particularly when estimating K_{ON}. The reason is that the K_{ON} estimation experiments lasted more time and the oxygen transfer effect became more important.

K_O values neglecting the DO probe time response were also estimated to assess the effect of this parameter. The results showed that neglecting the DO probe time response implied a significant underestimation of the K_O values because the values obtained were K_{OA} = 0.49 ± 0.02 mg O_2/L and K_{ON} = 1.640 ± 0.01 mg O_2/L. This response time was so important because the experimental profiles showed a sudden and sharp decrease which is faster than the time response of the probe.

In relation to the values of the K_O, the value of K_{ON} obtained was more than twice times the value of the K_{OA}. This indicated that the nitratation step was more influenced by oxygen limitations than the nitritation step. According to these values, one could evaluate which DO set point would be more favourable to accomplish partial nitrification.

This effect is shown in Figure VI.C6, where a simulation of the percentages of the maximum nitritation and nitratation rates achieved at different DO concentrations are plotted. For example, for a DO value of 2 mg DO/L (typical WWTP setpoint), the nitritation rate would be reduced to a 74 % of its maximum rate without limitations and the nitratation rate would be reduced down to 53 % of the maximum nitratation rate. Once this ratio is known, the value of both the maximum nitritation and nitratation rates should be calculated as a function of the operational conditions (such as temperature and pH) to estimate the operational nitritation and nitratation rates in the system.

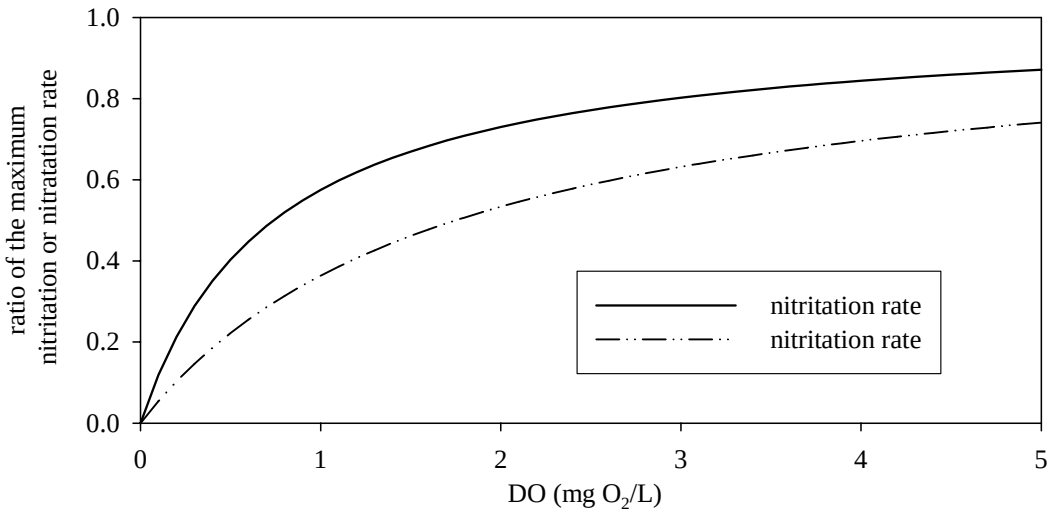

Figure VI.C6 Simulation of the nitritation and nitratation rate as function of DO concentration for K_{OA} = 0.74 mg O_2/L and K_{ON} = 1.75 mg O_2/L.

As can be observed, the lower the DO value, the more the nitritation is favoured in front of nitratation because, at low DO values, the effect of the K_O is more significant in the second step. Apparently, an optimal operation procedure to achieve partial nitrification would require low DO values (assuming that the values of both the maximum nitritation and nitratation rates are close). Moreover, the aeration costs will diminish while decreasing oxygen setpoint. However, low DO values also imply low nitrification rates and, hence, larger reactor volumes. After all, a balanced decision should be made taking into account all these features.

VI.C.4 Significance of oxygen limitations in respirometric batch experiments

An example of the oxygen limitation effect upon respirometric batch experiments is shown to explore the importance of this limitation when interpreting the measured OUR profile. In experiment VI.C5, a pulse of 10 mg N-NH_4^+/L was added with a low airflow so that, when the biomass consumed at its maximum rate, the DO in the reactor dropped until quite low values. Both the DO and the OUR profiles are plotted in Figure VI.C7.

Table VI.C6 Experiment VI.C5

EXPERIMENT VI.C5	Significance of oxygen limitation
Equipment	LFS respirometer (V_0 = 0.8 L)
pH	7.5
Temperature	25 ºC
Acid used	HCl = 0.25 M
Base used	NaOH = 0.25 M
Pulses	10 mg N-NH_4^+ (t=78 min) → 12.5 mg N-NH_4^+/L

As can be seen in the figure below, the OUR value did not instantaneously reach the maximum value after the ammonium pulse was added (t=78 min), but increased progressively. This transient period to reach the maximum OUR value known as acceleration is already discussed in Chapter VI.A. As this transient period was finishing, a maximum peak was attained and, then, the OUR decreased down to steady value as a consequence of oxygen limitations. The OUR value remained stable (around 2.2 mg O_2/L/min) as long as the DO did not change (i.e. there were no ammonium limitations).

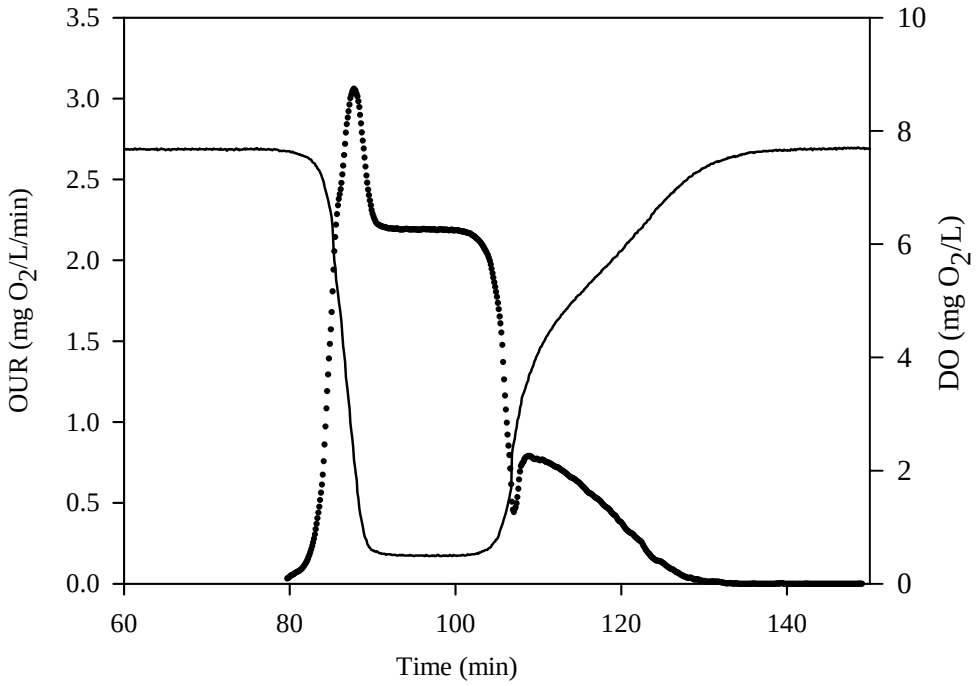

Figure VI.C7 Experimental DO and OUR profiles obtained with 12.5 mg N-NH_4^+/L and low airflow to cause oxygen limitation.

Hence, this initial unusual sharp pointed peak observed in the first shoulder of the OUR profile should not be attributed to experimental error, as it was related to oxygen concentration effluent. Similar (but smaller) sharp peaks can be obtained in respirometric batch experiments when the DO reaches values lower than 3 (Figure VI.C3). The K_{OA} value found in this work (0.74 ± 0.02 mg O_2/L) is in agreement with this observation.

In addition, the oxygen limitation effect could also be observed in the second shoulder of the OUR profile (nitratation step). When the DO level was at its lowest value (around 0.5 mg O_2/L), this step was extremely limited and, afterwards, as the DO rose because the nitritation step finished, the OUR related to the nitratation step increased considerably. The fact that the nitratation step was more sensible to oxygen limitations is in agreement with the K_O values previously estimated (K_{ON} = 1.75 ± 0.01 mg O_2/L).

Finally, the dependence of these unusual peaks on the oxygen limitations was simulated. Four different simulations were run with the same initial pulse addition (30 mg N-NH_4^+/L) and different k_La values so that the air transfer and the bottom DO level were higher in each simulation. The two-step nitrification model described in Chapter VI.A with standard parameters and a transient period of 1.3 min was used for simulations. The DO and OUR profiles obtained (Figure VI.C8) showed that the sharp peak observed in the first shoulder disappeared as the oxygen limitations were reduced (higher k_La), Moreover, the higher the k_La, the faster the pulse was consumed because both the nitritation and the nitration rates were not as much oxygen limited.

The specific OUR profiles related to the nitritation step and to the nitratation step are also depicted separately. The effect of oxygen limitations in the second step was clearly seen, mainly in the simulation with the lowest k_La value. In this simulation, the behaviour of this second shoulder was very close to the one experimentally observed (Figure VI.C8).

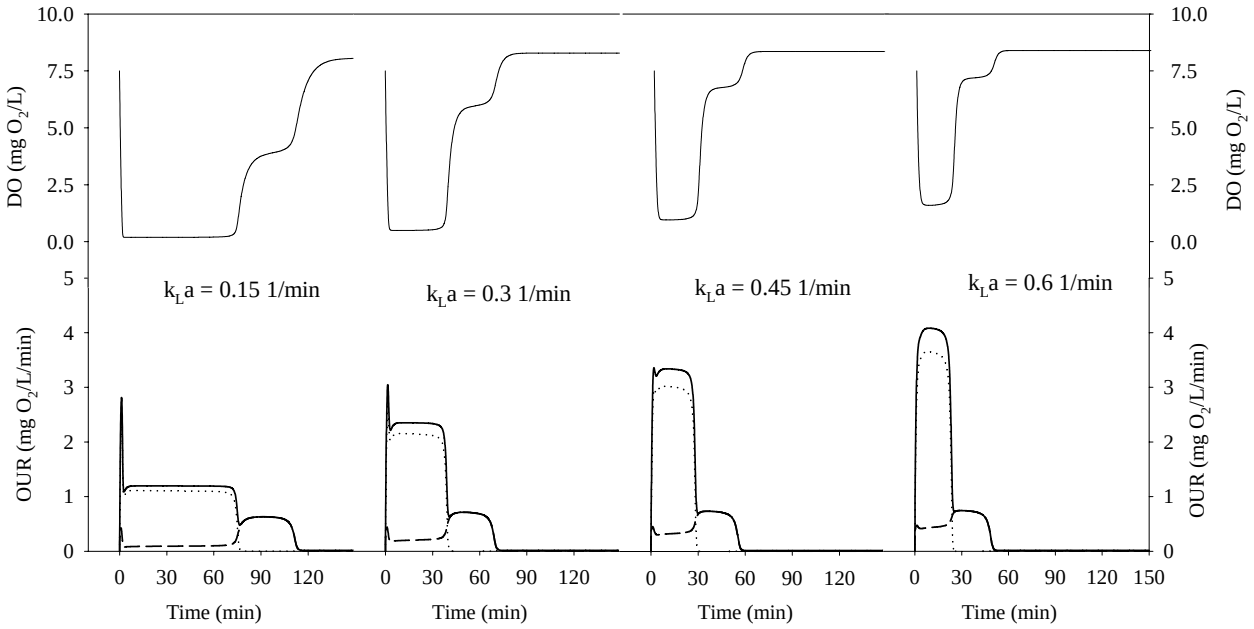

Figure VI.C8 Simulations of different ammonium pulses (30 mg N-NH_4^+/L) at different k_La values. DO and OUR profile are depicted with solid lines and the OUR related to nitritation and nitratation are depicted in dotted and dashed lines respectively.

CHAPTER VI.C CONCLUSIONS

- An extension of the procedure employed by Wiesmann *et al.*, 1994 for the K_{ON} estimation was employed for both K_{OA} and K_{ON} estimation. The results obtained were K_{OA} = 0.74 ± 0.02 mg O_2/L and K_{ON} = 1.75 ± 0.01 mg O_2/L.

- Hence, the nitratation step is more influenced by oxygen limitations than the nitritation step. Depending on the DO set point chosen and taking into account the maximum nitritation and nitratation rate, one can expect to achieve partial nitrification by favouring the nitritation step in front of the nitratation step.

- These K_O values are considerably higher than the default ones used in the classical ASM1 (Henze *et al.*, 2000). This fact could influence the estimated values of μ_{MAX} and K_S from respirometric batch experiments using 0.4 as K_O.

- It has been demonstrated that oxygen transfer from atmosphere should be taken into account when using open and stirred systems such as the one used in this work. Otherwise, the K_O values would be overestimated.

- To take into account this oxygen transfer, the volumetric oxygen transfer constant form atmosphere (k_La^{SUP}) was calculated by measuring the endogenous OUR value at different surface to volume ratios in the reactor.

- The DO probe time response was also estimated for a proper K_O estimation. Neglecting the DO probe time response implied an underestimation of the K_O values because of the sharp experimental DO decrease which is faster than the time response of the probe.

CHAPTER VI.D

Quantification of inorganic carbon limitations upon nitrification

This chapter is in preparation for submission to Water Research

ABSTRACT

Nitrification is a two step process which involves two different biomass populations: ammonia oxidising biomass (AOB) and nitrite oxidising biomass (NOB). Both biomasses are autotrophic (i.e. their carbon source is inorganic). Therefore, a deficit of this substrate should result in a decrease of the process rate. This limitation has often been omitted for modelling purposes since it is difficult to have a scenario with inorganic carbon limitations in real systems. However, the recent technology advances have brought new scenarios in biological nitrogen removal where these limitations should be considered. This chapter examines the TIC limitation through respirometric and titrimetric techniques. The evolution of the TIC is indirectly followed with titrimetry and the process rate is followed with both respirometry and titrimetry. The experimental results obtained show that NOB biomass could not be carbon limited in the working range of TIC concentration studied. On the other hand, AOB was limited by TIC at concentrations lower than 3 mM.

VI.D.1 Motivations for a carbon limitation study on nitrification

The populations involved in the nitrification process (AOB and NOB) are autotrophic. Hence, their carbon source must be inorganic and a deficit of this substrate should result in a decrease of the process rate. Likewise other substrates (i.e. ammonium, nitrite or oxygen) its limitation should be studied and taken into account in view of process modelling. The carbon limitation issue is linked to the alkalinity requirements of the system to buffer the acidification of the media due to the nitritation process. Hence, the bicarbonate is used for both buffering and growing purposes. In this sense, Wett and Rauch (2002) pointed out that carbon limitations could be one of the causes of the common knowledge that growth and activity of nitrifying bacteria decreases dramatically below neutrality. The equilibriums of the carbonic acid are depicted in equation VI.D1. Carbonic acid is depicted as H_2CO_3* to indicate that this acid is very unstable and it is mostly found as CO_2 +H_20. The pKa of H_2CO_3* is 6.36 and the pKa of HCO_3^- is 10.35 (for pure water). Hence, under conditions close to neutrality, most of the total inorganic carbon (TIC) present in the system is in HCO_3^- form. As can be observed, a huge decrease in the pH would imply an equilibrium displacement from bicarbonate to carbonate.

$$CO_2(g) + H_2O \Leftrightarrow H_2CO_3 \Leftrightarrow H^+ + HCO_3^- \Leftrightarrow H^+ + CO_3^{2-} \qquad \text{(VI.D1)}$$

The TIC limitation is not as largely studied in the literature as the case of oxygen or N-substrate (ammonia or nitrite). This limitation has often been omitted since it was difficult to find a scenario with TIC limitation in real systems. For example, in a conventional WWTP, the amount of CO_2 produced due to the oxidation of COD (heterotrophic activity) is high enough for the autotrophic bacteria to grow.

However, nowadays, biological nitrogen removal systems have evolved from the classical nitrification/denitrification systems in view of treating more efficiently different N-loaded wastewaters. For example, Carrera *et al*. (2003, 2004b) studied the case of industrial wastewaters with low COD/N ratios. They developed a single-sludge and a two-sludge system for treating high N-strength wastewaters which contained less alkalinity than the stoichiometrically necessary. This lack of alkalinity caused ammonium accumulation and, consequently, ammonia inhibition. Hence, the pH was controlled using sodium carbonate which avoided carbon limitations.

The importance of TIC concentration is emphasized in high N-strength wastewaters such as the rejection water of digested sludge which may contain 15-30 % of the total nitrogen entering to the WWTP. Some of these rejection wastewaters practically do not have COD (e.g. Fux *et al.*, 2002 or Janus and van der Roest, 1997) and, in others, the ammonium nitrogen concentration can be 1, 2 or 4 times higher than the COD (e.g. Lai *et al.*, 2004). Other examples of high ammonia loaded wastewaters are landfill leachate and piggery wastewater (Wett and Rauch, 2002).

One of the recent advances in the biological nitrogen removal field is the combination between the SHARON® (Hellinga *et al.*, 1998, 1999) and the anammox® processes (van Loosdrecht and Jetten, 1998). The combination of these processes represents an upgrading of the classical nitrification/denitrification process since no organic matter is required for biological nitrogen removal. When these processes are combined, the SHARON® reactor (where partial nitrification is occurring) is used to provide the feed of the anammox® reactor (where ammonium is oxidised with nitrite as electron acceptor by anammox® bacteria). According to the stoichiometry, only half of the ammonium entering to the SHARON® reactor should be oxidised to nitrite. Van Donguen *et al.* (2001) or Fux and Siegrist (2004) showed that the ratio of nitrite/ammonium at the outlet of a SHARON® reactor is extremely dependent on the ratio of ammonium/alkalinity in the inlet of the reactor. Moreover, these works declared that if no base (alkalinity) was added to the process, the alkalinity of the wastewater could be low enough so that only part of the ammonium was oxidised. Hence, as can be observed, these systems work under carbon limitations, and a better knowledge of this limitation process is required.

Few studies appear in the literature investigating the inorganic carbon limitation in nitrification. The reference in the activated sludge modelling, ASM2 (Henze *et al.*, 2000), predicts a limitation of alkalinity upon nitrification with Monod kinetics (K_{ALK} = 0.5 mmol HCO_3^-/L). Byong-Hee *et al.*, (2000) studied the effect on nitrifying biofilm which worked on continuous-flow operation mode, by which TIC was supplemented in order to stimulate the growth of autotrophic nitrifying bacteria. Wett and Rauch (2002) studied the kinetics of carbon limitation with data from real WWTP rejection-water and developed a new sigmoidal kinetic model to take into account the carbon limitation effect together with other nitrification inhibitions.

The aim of this chapter is to quantitatively assess the effect of carbon limitations on both steps of nitrification and to obtain the dependence of the process on the TIC concentration.

VI.D.2 Evolution of TIC on aerated systems

For a proper study of carbon limitations, the evolution of TIC on aerated systems should be perfectly described. This evolution depends on the physical equilibrium between the gas and liquid phases, the chemical equilibriums of the carbonic acid and the biological carbon production/consumption rate. Equation VI.D2 depicts the CO_2 balance in the liquid phase of an aerated bioreactor:

$$\frac{d(S_{CO2} \cdot V)}{dt} = CTR \cdot V + CPR \cdot V \qquad \text{(VI.D2)}$$

where S_{CO2} stands for the CO_2 concentration in the liquid phase (mol CO_2/L)

CPR for the Carbon Production Rate (mol CO_2/L/min),i.e. CO_2 produced or consumed biologically.

CTR stands for Carbon Transfer Rate (mol CO_2/L/min), i.e. CO_2 transferred though the gas-liquid interphase to the liquid phase.

The CTR depends on a constant and a driving force [eq. VI.D3]:

$$CTR = k_L a_{CO2} \cdot (S^*_{CO2} - S_{CO2}) \quad \text{(VI.D3)}$$

Where k_La_{CO2} = CO_2 mass transfer constant (1/min).
S^*_{CO2} = saturation CO_2 concentration (mol CO_2/L)

The value of S^*_{CO2} is usually lower than S_{CO2} and stripping occurs. Equation VI.D2 can be converted to equation VI.D4 in the case of endogenous conditions.

$$\frac{d(S_{CO2} \cdot V)}{dt} = k_L a_{CO2} \cdot (S^*_{CO2} - S_{CO2}) \cdot V + CPR_{END} \cdot V \quad \text{(VI.D4)}$$

The CO_2 will be stripped from a continuously aerated system until the steady state is reached. At this point, S_{CO2} will be constant, and the value of CPR will be equal to CTR [eq. VI.D5].

$$\left(\frac{dS_{CO2} \cdot V}{dt}\right)_{SS} = 0 \longrightarrow k_L a_{CO2} \cdot (S_{CO2}{}^{*} - S_{CO2}{}^{SS}) = CPR_{END} \quad \text{(VI.D5)}$$

Under endogenous conditions the amount of CO_2 produced (CPR_{END}) is very similar to the amount of oxygen consumed (OUR_{END}). This premise is detailed in Section VI.A.2.6, where the stoichiometry of the endogenous process is described. As the degree of reduction of the biomass (γ_X) is usually around 4, then the molar ratio of CO_2 produced versus O_2 consumed (known as respiratory quotient) is close to 1. Hence, when the system is aerated until it reaches steady-state conditions, the value of dissolved CO_2 (S^{SS}_{CO2}) at this point can be calculated as [eq. VI.D6].

$$\frac{d(S_{CO2} \cdot V)}{dt} = 0;\ S^*_{CO2} + \frac{CPR_{END}}{k_L a_{CO2}} = S^{SS}_{CO2} \quad \text{(VI.D6)}$$

It can be argued that the stoichiometry of the endogenous process is only an approximation and that part of the oxygen may be consumed without CO_2 production. Hence, the assumption that CPR_{END} is equal to OUR_{END} may overestimate the $S_{CO2}{}^{SS}$ value. The value of pH at the steady state can be calculated using the values of the carbonic acid-carbonate equilibrium according to equation VI.D7.

$$pH^{SS} = -\log \frac{K_1 \cdot S^{SS}_{CO2}}{S^{SS}_{HCO3}} \quad \text{(VI.D7)}$$

The work of Ficara *et al.*, (2003) was one of the first successful attempts to use titrimetry in view of activated sludge monitoring. They developed a titrimetric equipment which worked at the pH value reached in the steady state when the system was aerated (pH^{SS}). According to equations VI.D6 and VI.D7, this pH^{SS} depends on the CPR_{END} value and on the mass transfer efficiency. Hence, they performed experiments with variable pH set point. In fact, depending on the experimental conditions they found a range of pH^{SS} from 7.8 and 8.5.

However, the pH in the experiments of this thesis was controlled at a certain setpoint lower than pH^{SS} (the pH setpoint, pH^{SP}, was usually 7.5). Figure VI.D1 shows a schematic representation of the carbonic acid-bicarbonate equilibrium. This graphic represents S_{CO2} versus S_{HCO3} for a certain pH value.

Each pH value is represented by a different line according to equation VI.D8.

$$S_{CO2} = \frac{\left(10^{-pH}\right)}{K_1} \cdot S_{HCO3} \qquad \text{(VI.D8)}$$

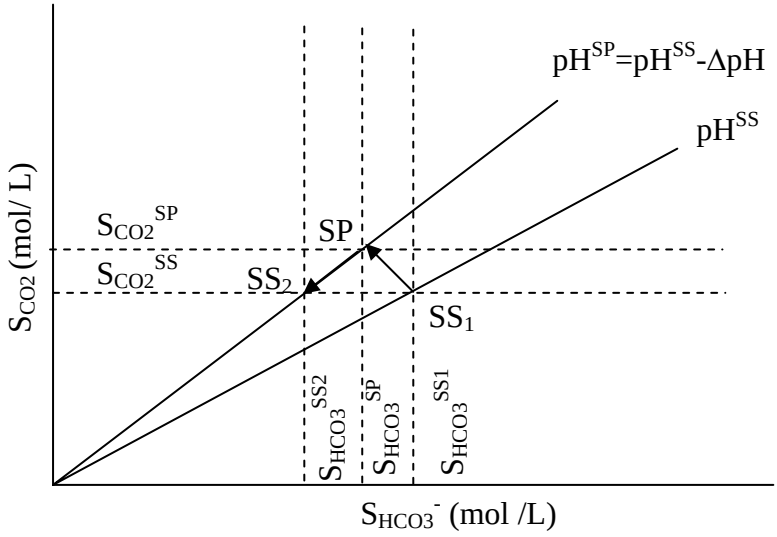

Figure VI.D1 Schematic representation of the carbonic acid-bicarbonate equilibrium for a dynamic process.

SS_1 represents the steady state point reached when the system is continuously aerated without pH control. It is assumed that the CPR_{END} value is constant for this discussion. Afterwards, once the pH is controlled at 7.5, the system evolves to the point SP. This evolution is indicated with an arrow (from SS_1 to SP). At this value, the value of S_{CO2} (S_{CO2}^{SP}) is higher than the value of S_{CO2}^{SS} and then, S_{CO2} is stripped. This stripping implies a loss of TIC (in terms of moles/L/min) from the system. This loss is done maintaining the proportions fixed by the equilibrium (i.e. following the corresponding pH line). This loss is indicated with an arrow (from SP to SS_2). The second steady state point (SS_2) is attained when the S_{CO2} value corresponds again to S_{CO2}^{SS}. At this point, the value of CTR is again equal to CPR_{END}. SS_1 and SS_2 have the same S_{CO2} concentration but different S_{HCO3} and pH values. In this case, S_{HCO3}^{SS1} is lower than S_{HCO3}^{SS2} due to the stripping.

In short, the amount of S_{CO2} in the steady state is independent of the initial inorganic carbon and the pH chosen. The value of S_{CO2}^{SS} only depends on the CO_2 efficiency transfer (k_La_{CO2}), the concentration of CO_2 in the gas phase (S^*_{CO2}) and the CPR_{END} value.

The value of S^{SS}_{CO2} is very low. For example, a common value obtained in this thesis with default parameters is 0.01 mM. However, the affinity of the biomass for the carbon substrate is very high and it could be possible that this steady state value was high enough to avoid carbon limitations. For this reason, an alternative system to reduce S_{CO2} was tested. The system was aerated with synthetic air without CO_2 to further reduce the concentration of bicarbonate in the medium. This system provided lower S^{SS}_{CO2} values and the carbon limitations could be better studied. In this scenario the S^{SS}_{CO2}, can be calculated as equation VI.D9.

$$\frac{CPR_{END}}{k_L a_{CO2}} = S^{SS}_{CO2} \qquad \text{(VI.D9)}$$

Experiment VI.D1 (Table VI.D1) shows the typical accumulated acid and pH profiles obtained when the system was aerated with synthetic air for an overnight to reach steady state conditions. As can be observed, the lower the TIC is, the lower the buffering

capacity of the system and the higher the impact of acid dosage on pH. To avoid these high decreases in the pH value, the amount of acid dosage should be variable (decreasing in time). A control strategy could be linking the amount of acid dosage with the decrease produced by the last dosage. However, as the objective of the overnight aeration was to reach steady state, this control was not implemented.

Table VI.D1 Experiment VI.D1

EXPERIMENT VI.D1	Accumulated acid and pH in an aerated reactor
Equipment	LFS respirometer (V_0 = 1 L)
pH	7.5
Temperature	25 ºC
Acid used	HCl = 0.5 M
Pulses	-

Figure VI.D2 shows the experimental profiles obtained in experiment VI.D1. It can be observed that more than ten hours are required to reach the steady state. At this point (i.e. acid dosage is zero) S_{CO2} is not zero but a value calculated according to equation VI.D9 (i.e. S_{CO2}^{SS}).

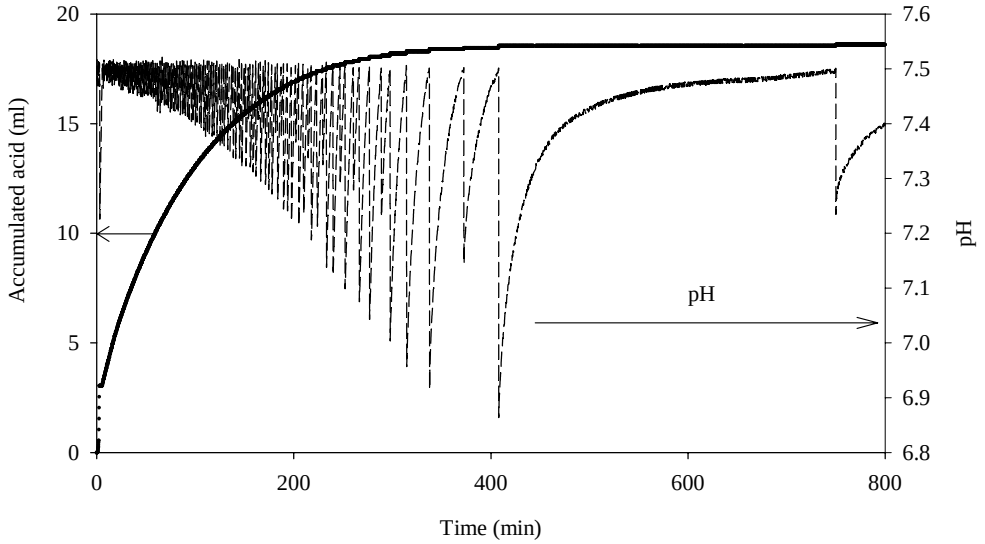

Figure VI.D2 Experimental pH and accumulated acid profiles for experiment VI.D1

Experiment VI.D2 (Table VI.D2) was conducted to examine how synthetic aeration reduced the value of S_{CO2}^{SS}. This experiment consisted of aerating the system with synthetic air until the steady state was reached. At this point, the aeration was switched to conventional air (i.e. with 0.036 % of CO_2). Both airflows were identically, since an airflow meter was used.

Table VI.D2 Experiment VI.D2

EXPERIMENT VI.D2	Differences between synthetic and conventional aeration
Equipment	LFS respirometer (V_0 = 1 L)
pH	7.5
Temperature	25 ºC
Base used	NaOH = 0.5 M
Pulses	-

Figure VI.D3 shows the experimental profiles of pH and accumulated base obtained in experiment VI.D2. Before switching to conventional aeration, S_{CO2} was very low (equation VI.D9). After the switch, the S_{CO2}* became higher than S_{CO2} and carbon dioxide was transferred from the gas phase to the liquid phase (i.e. CO_2 absorption). Hence, as the pH of the media was 7.5, the “entering” inorganic carbon was rapidly transformed to

bicarbonate resulting in proton release to the media. Base dosage was required to balance this carbon absorption.

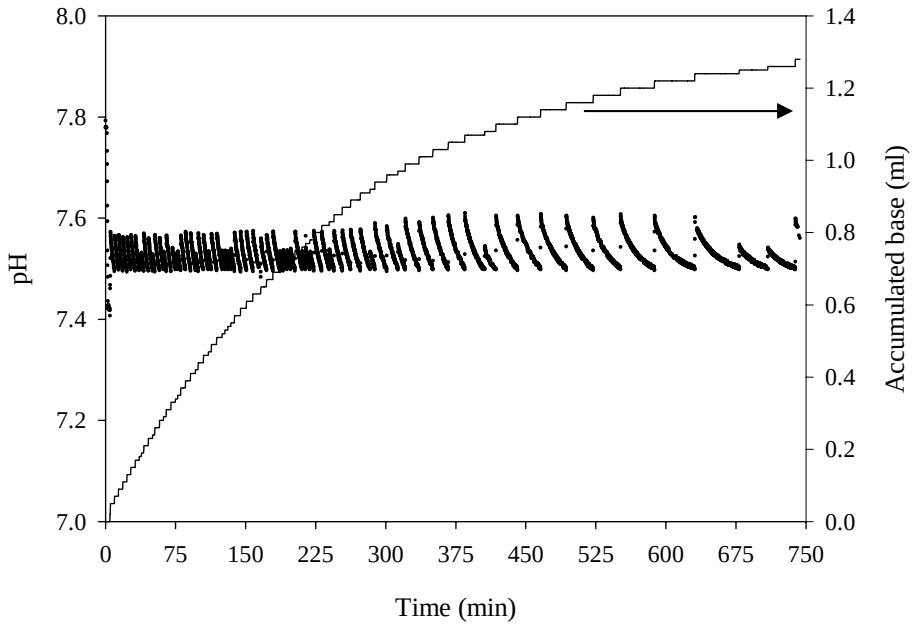

Figure VI.D3 Experimental pH and accumulated acid profiles for experiment VI.D2

As can be observed, the amount of base added was almost 1.3 ml which represents 0.65 mmols of NaOH. These are also the moles of CO_2 absorbed and, as one mol of OH^- is required to balance each mol of bicarbonate formed, 0.65 mmol/L is approximately the difference between S_{CO2}^{SS} with synthetic and with conventional aeration for this particular experiment. As can be observed below, this is a significant difference.

VI.D.3 Carbon limitations upon nitrification

Experiment VI.D3 (Table VI.D3) was conducted to assess whether the system could be carbon limited with synthetic air aeration or not. The experiment was performed in the LFS respirometer with nitrifying enriched biomass and it consisted of aerating with synthetic air (i.e. without CO_2) for a long period of time. Each day a pulse of ammonium was added to assess the nitrifying activity. This continuous aeration was planned to last the time necessary to observe carbon limitations (i.e. decrease in the OUR).

Table VI.D3 Experiment VI.D3

EXPERIMENT VI.D3	Assessment of carbon limitations with ammonium pulses
Equipment	LFS respirometer (V_0 = 1 L)
pH	7.5
Temperature	25 ºC
Acid used	HCl = 0.5 M
Pulses	3 x 10 mg $N\text{-}NH_4^+$ (days 1,2 and 3)
	1 g $NaHCO_3$ (12 mmols HCO_3^-) at day 4
	5 x 10 mg $N\text{-}NH_4^+$ (day 4)

Figures VI.D4(a-d) show the experimental OUR profiles obtained in experiment VI.D3. As can be observed, a high decrease in the process rate was observed after three days of synthetic aeration. This decrease was due to TIC limitations since when a pulse of sodium bicarbonate was added (fourth day), the system recovered its maximum nitrification rate again and acid dosage was required to balance the proton consumption due to CO_2 stripping (Figure VI.D4d). The pulse of bicarbonate was not extremely high and the carbon limitations appeared again in the same day 4 as bicarbonate was being depleted.

In addition, the accumulated acid profile in the fourth day shows that the CO_2 stripping was fast enough to balance the protons produced in the nitritation in the first three pulses and base dosage was only required in the last two pulses.

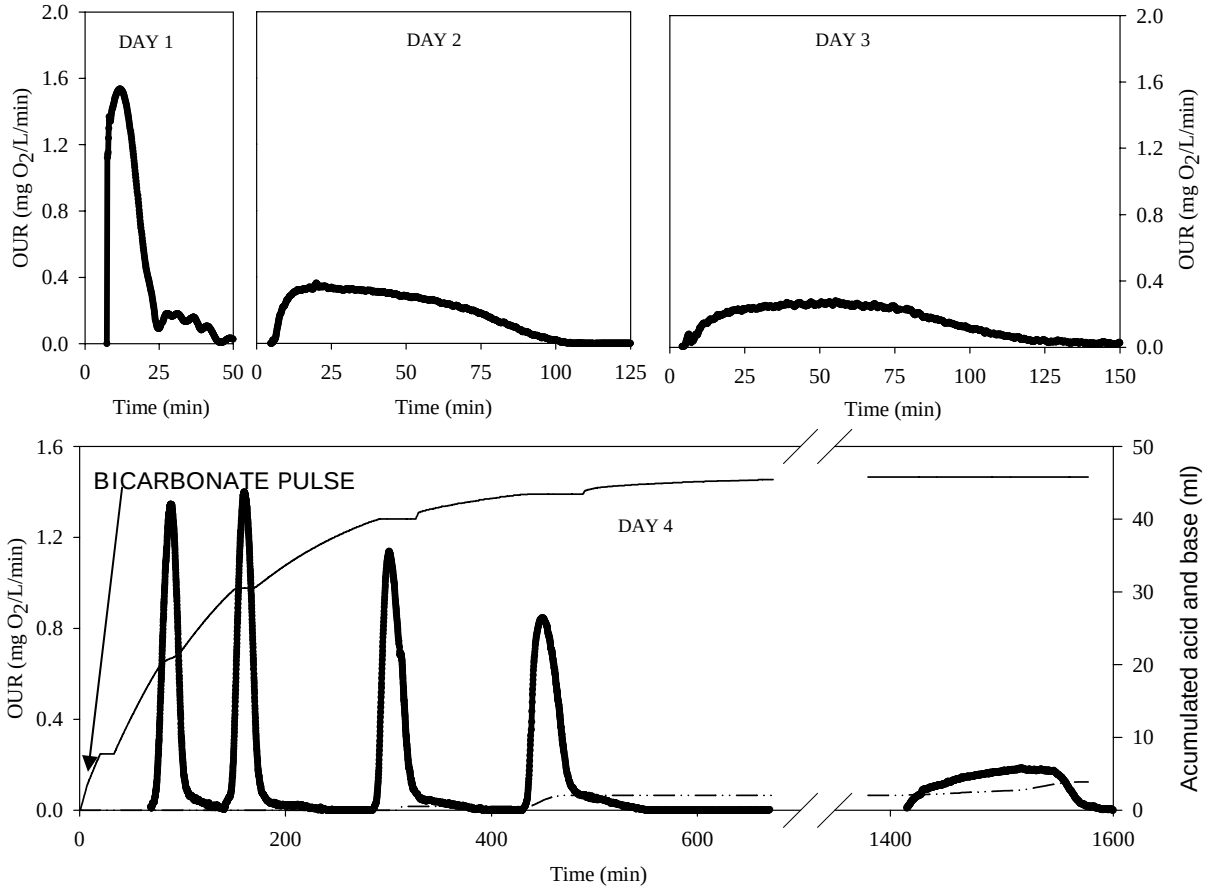

Figure VI.D4 Experimental profiles of experiment VI.D2: OUR (dotted), acid dosage (solid) and base dosage (dash-dotted).

The same experiment was conducted with nitrite addition instead of ammonium (experiment VI.D4). The biomass was left overnight with synthetic aeration and a pulse of bicarbonate was added. Several pulses of nitrite were added to the system and OUR and accumulated acid was measured.

Table VI.D4 Experiment VI.D4

EXPERIMENT VI.D4	Assessment of carbon limitations with nitrite pulses (I)
Equipment	LFS respirometer (V_0 = 1 L)
pH	7.5
Temperature	25 ºC
Acid used	HCl = 0.5 M
Pulses	0.5 g $NaHCO_3$ (~6 mmoles HCO_3^-)
	4 x 10 mg N-NO_2^-

Figure VI.D5 depicts the experimental profiles obtained. As can be observed, no TIC limitations are observed, and the OUR profiles are practically identical. These would indicate the NOB requires much lower TIC concentrations to be inhibited. This fact is not surprising since differences in substrate affinity between both populations have already been observed (i.e. oxygen affinity – see previous chapter). The acid dosage in experiment VI.D4 is only influenced by the stripping process since the nitratation neither consumes nor produces protons.

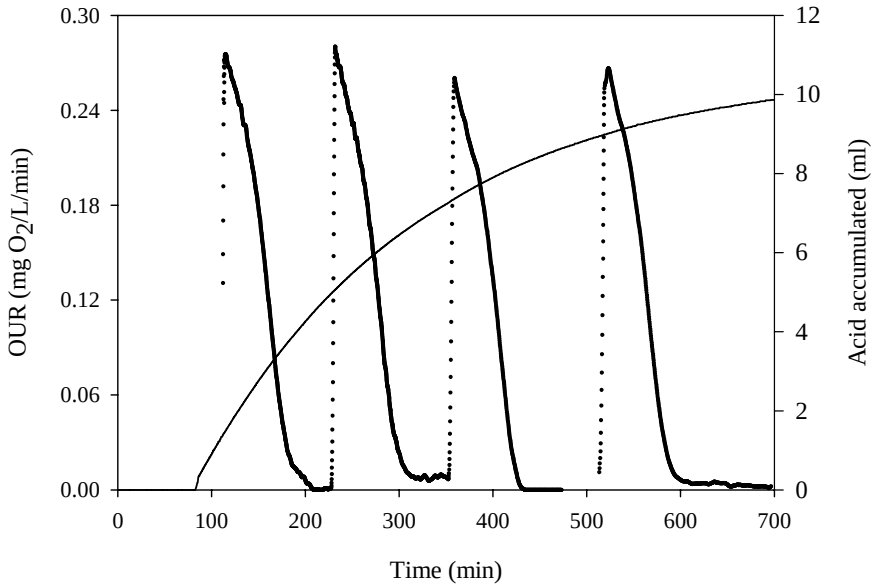

Figure VI.D5 Experimental profiles of experiment VI.D4: OUR (dotted), acid dosage (solid)

The fact that NOB biomass was not inhibited by carbon limitations at the same range of AOB was supported with experiment VI.D5 (Table VI.D5), where several pulses of nitrite where added to a biomass previously aerated with synthetic aeration. The differences with respect to the previous experiment were that the biomass was diluted to its half and no initial pulse of bicarbonate was added and, the TIC concentration was very low along the experiment.

Table VI.D5 Experiment VI.D5

EXPERIMENT VI.D5	Assessment of carbon limitations with nitrite pulses (II)
Equipment	LFS respirometer (V_0 = 1 L)
pH	7.5
Temperature	25 ºC
Acid used	HCl = 0.5 M
Pulses	4 x 5 mg $N\text{-}NO_2^-$

Figure VI.D6 displays the experimental OUR profiles. The conclusion of this experiment is that NOB is not TIC limited in this working range. The amount of TIC present in the liquid due to the carbon production of the biomass is enough to ensure NOB growth.

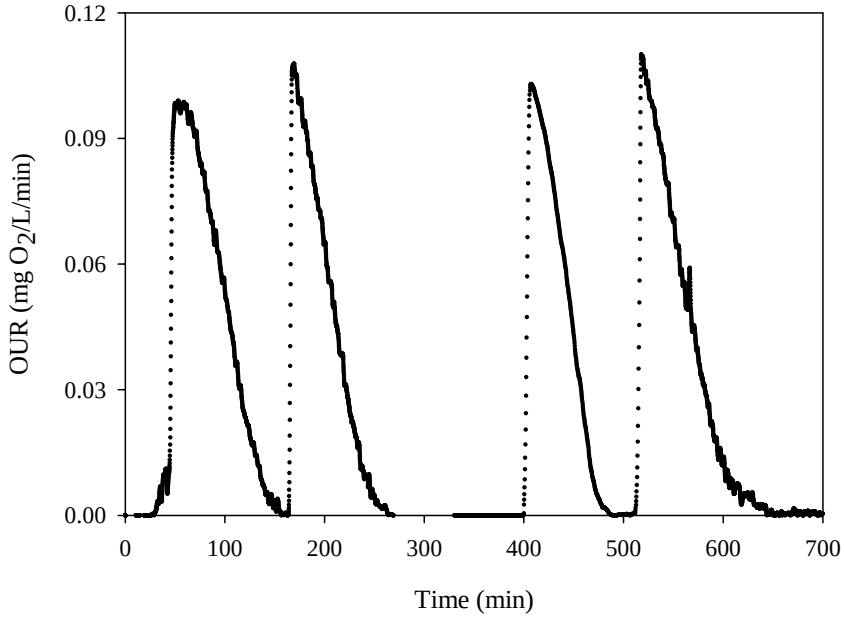

Figure VI.D6 Experimental OUR profiles of experiment VI.D5

VI.D.4 Assessment of carbon limitations kinetics

VI.D.4.1 USING TITRIMETRY FOR TIC ESTIMATION

Once it was proved that the system could be carbon limited, a set of experiments was planned to quantify this limitation. For this aim, the evaluation of the nitrification rate at different TIC values was required; however, measuring TIC was not that simple, particularly at the low TIC levels necessary in this work. In addition, sample volumes of more than 10 ml were required and the measurement detection limit of the equipment used was too high for our purposes. Hence, an indirect measurement of TIC was searched using the titrimetric measurements. The basis of this measurement is:

1. In the periods with neither ammonia nor nitrite oxidation, there is only acid addition due to CO_2 stripping. Each mole of acid added corresponds to a mole of carbon dioxide stripped.
2. 1.98 moles of protons are produced and released to the medium for each mole of $N\text{-}NH_4^+$ taken up and 5.94 moles of CO_2 are consumed for growth purposes for each gram of $N\text{-}NH_4^+$ taken up (see model stoichiometry Chapter VI.A).

Hence, if the initial TIC value is known, the TIC concentration in time can be approximated using the three previous statements. Experiment VI.D6 (Table VI.D96) was performed with pure water to link TIC and titrimetry without any interferences. Figure VI.D7 shows the experimental TIC measurements together with the TIC estimation measurements according to equation VI.10 for an aerated system. As can be observed TIC is reasonable well predicted.

Table VI.D6 Experiment VI.D6

EXPERIMENT VI.D6	Linking TIC to titrimetry
Equipment	LFS respirometer (V_0 = 1 L)
pH	7.5
Temperature	25 ºC
Acid used	HCl = 0.35 M
Base used	NaOH = 0.3 M
Pulses	1g $NaHCO_3$ (t = 20 min)

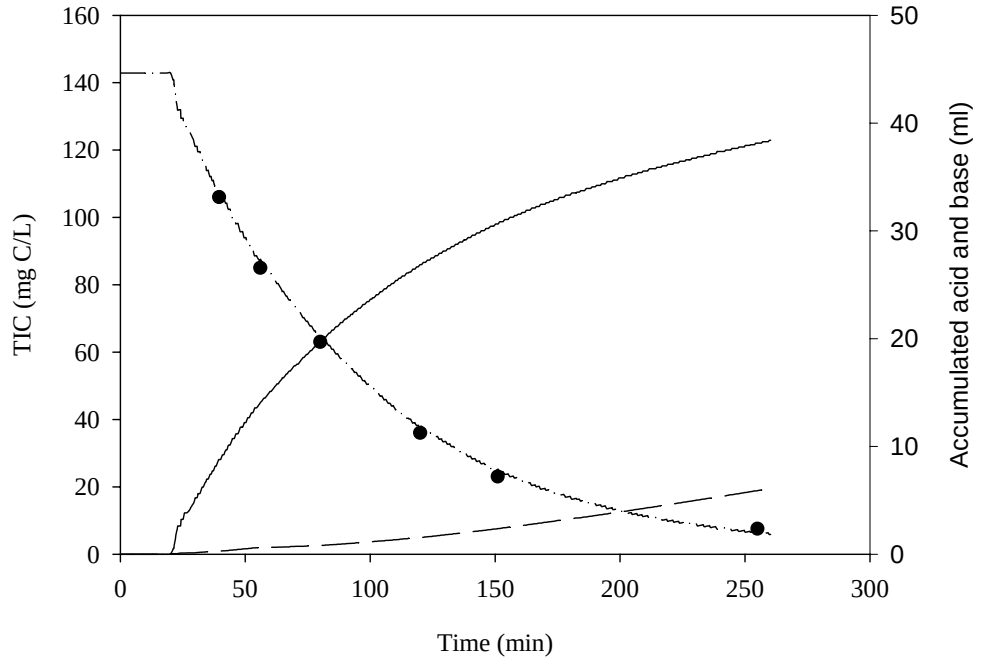

Figure VI.D7 TIC predicted (dash-dotted line) versus TIC measured (dotted) for an aerated bioreactor. Accumulated acid (solid line) and base (dashed line).

VI.D.4.2 OUR_{MAX} versus TIC: TIC ESTIMATION METHODOLOGY

The set of experiments VI.D7 (Table VI.D7) consisted of measuring maximum OUR values at different TIC values. In each experiment, the biomass was left only with synthetic aeration overnight to reach steady state conditions (likewise Figure VI.D1). At this point, a known pulse of sodium bicarbonate was added and stripping was observed. Then, several pulses of ammonium were added which had different OUR_{MAX} values depending on the TIC concentration. The TIC concentration in a certain moment was estimated using the amount of acid and base dosage data. Four experiments with different initial bicarbonate concentrations were conducted. In these experiments OUR, acid and base dosage and the initial bicarbonate added were measured.

Table VI.D7 Experiment VI.D7

EXPERIMENT VI.D7	Assessment of carbon limitation kinetics
Equipment	LFS respirometer (V_0 = 0.95 L)
pH	7.5
Temperature	25 ºC
Acid used	HCl (0.5 M / 0.1 M)
Base used	NaOH (0.5 M / 0.2 M)
Pulses	9 x 10 mg N-NH_4^+
	0.5 / 0.1 / 0.05/ 0.02 g $NaHCO_3$

Figure VI.D8 shows an example of one of these experiments where OUR, accumulated base and accumulated acid were measured.

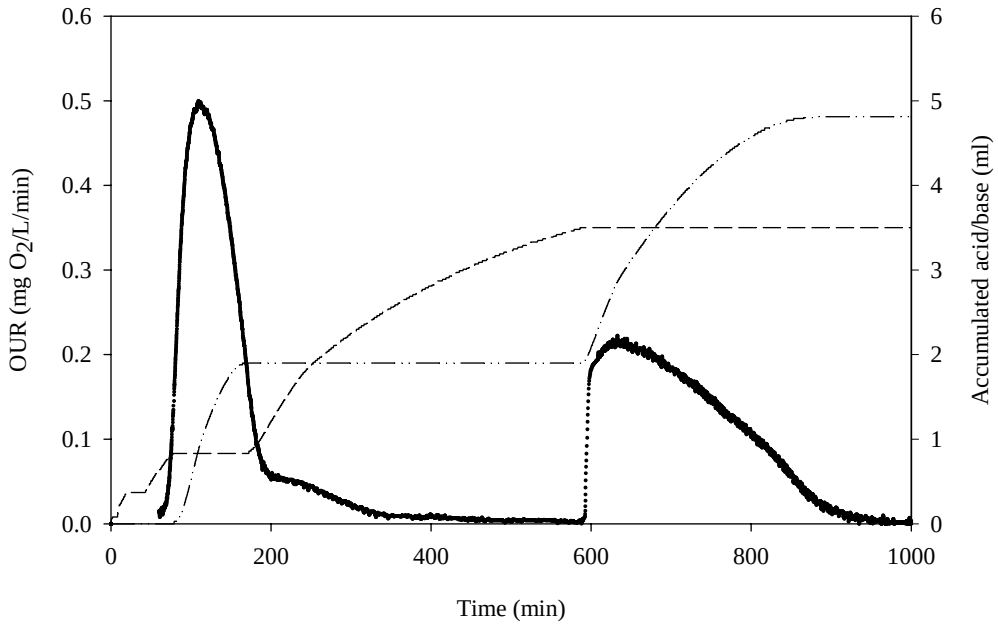

Figure VI.D8 Experimental profiles of one of the experiments of VI.D7: OUR (dotted), acid dosage (dashed) and base dosage (dash-dotted).

The value of TIC before each pulse was calculated taking into account several factors as shown in equation VI.D10

1. The initial TIC concentration before the bicarbonate pulse [eq. VI.D9].
2. The TIC concentration as sodium bicarbonate added in the pulse
3. The amount of acid and base dosage before the pulse
4. The amount of protons produced and CO_2 consumed due to previous ammonium pulses
5. The increase of volume due to acid/base/feed addition

$$TIC = \frac{TIC_{PRESENT} \cdot V_{INITIAL} + NaHCO_{3\ ADDED} - (H^{+}_{DOSAGE} + H^{+}_{PRODUCED} - OH^{-}_{DOSAGE}) - CO_{2\,CONSUMED}}{V_{FINAL}} \quad \text{(VI.D10)}$$

Table VI.D8 shows an example of equation VI.D10 application for the estimation of the TIC concentration of the second pulse of Figure VI.D8. The value of OUR_{MAX} is corrected for biomass concentration (VSS) and for oxygen limitations using the K_O values estimated in the previous chapter.

Table VI.D8 Example of TIC estimation during an experiment with several ammonium pulses

Parameter	Units	Value	Calculated as
Biomass (VSS)	mg VSS/L	800	Measured
Experimental OUR_{MAX}	mg O_2/L/min	0.21	Measured
Specific OUR_{MAX}	g O_2/g VSS/ min	0.26	Exp OUR_{MAX} / Solids
S_O	mg O_2/L	5.77	Measured
OUR_{MAX} (*)	g O_2/g VSS/ min	0.30	Specific $OUR_{MAX} \cdot (K_O + S_O)/S_O$
OUR_{END} (mg O_2/L/min)	mg O_2/L/min	0.0089	Measured
CPR_{END} (mmol CO_2/min)	mmol CO_2/L/min	2.5E-04	$OUR_{END} \cdot \gamma_X/8$
k_La_{O2}	1/min	0.25	Measured
k_La_{CO2}	1/min	0.23	$0.91 \cdot k_La_{O2}$
$TIC_{PRESENT}$	mmol CO_2/L	1.11E-03	CPR_{END}/k_La_{CO2}
$NaHCO_{3\ ADDED}$	g $NaHCO_3$	0.2	Known
$V_{INITIAL}$	L	0.95	Measured
$TIC_{INITIAL}$	mmol CO_2/L	2.38	$TIC_{ADDED}/84 \cdot 1000 + TIC_{PRESENT} \cdot V_{INITIAL}$
Accumulated Acid	ml	3.5	Measured
Accumulated protons	mmol H^+	1.75	Accumulated acid · Acid Conc (0.5 M)
Accumulated base	ml	1.9	Measured
Accumulated hydroxyls	mmol OH^-	0.95	Accumulated base · Base Conc (0.5 M)
Previous pulses	mg N	10	Measured
Previous proton produced(**)	mmol H^+	1.43	Previous pulses/10·1.98
Previous CO_2 consumed(**)	mmol CO_2	0.059	Previous pulses/1000·5.94
V_{FINAL}	L	0.955	Measured
TIC CONCENTRATION	mmol CO_2/L	0.097	equation VI.D10

(*) OUR_{MAX} is recalculated considering oxygen limitations with K_O = 0.74 mg O_2/L (see Chapter VI.C)
(**) The amount of proton produced and CO_2 consumed per mol of ammonium oxidised are calculated according to the model presented in chapter VI.A

Nine points were obtained using the methodology of TIC estimation proposed in equation VI.D10 which are plotted below in Figure VI.D10 (circle points). The profile obtained agrees with what it was expected since as the process rate decreases together with the TIC concentration. However, an alternative methodology was tested to obtain more experimental points and to validate the previous TIC estimation methodology.

VI.D.4.3 OUR_{MAX} versus TIC: DIRECT TIC METHODOLOGY

The direct TIC methodology was thought in order to have a direct measurement of TIC concentration. The set of experiments VI.D8 (Table VI.D9) also consisted of measuring maximum OUR values at different TIC values. In each of the experiments the biomass was left only with synthetic aeration overnight to reach steady state conditions. At this point, a pulse of nitrogen as ammonium was added, which was slowly consumed because of carbon limitations. Once the maximum rate was reached a pulse of known bicarbonate was added to the system and the OUR_{MAX} value increased sharply since carbon limitations were reduced. Five experiments with different bicarbonate concentrations were conducted.

Table VI.D9 Experiment VI.D8

EXPERIMENT VI.D8	Assessment of carbon limitation kinetics (II)
Equipment	LFS respirometer (V_0 = 0.95 L)
pH	7.5
Temperature	25 ºC
Acid used	HCl (0.5 M)
Base used	NaOH (0.5 M)
Pulses	5 x 10 mg N-NH_4^+
	0.03 / 0.02 / 0.015/ 0.01/0.0015 g $NaHCO_3$

Figure VI.D9 shows an example of OUR profile obtained using this methodology. As can be observed, the increase of OUR once the bicarbonate pulse was added is very evident.

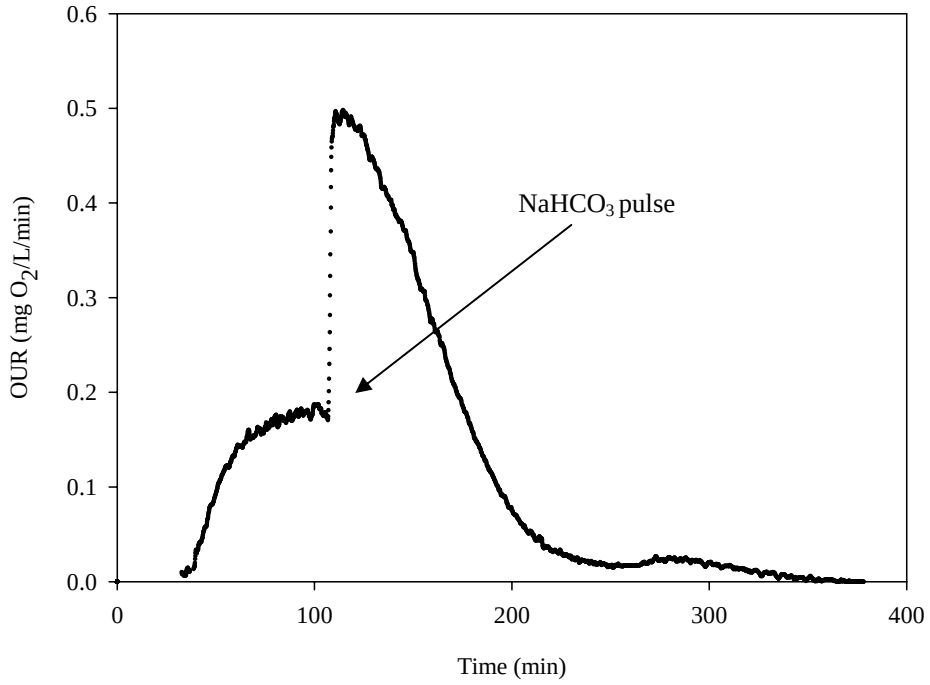

Figure VI.D9 Example of OUR profile of one experiment VI.D8

The TIC concentration for each pulse was calculated as the amount of TIC added with the pulse plus the initial TIC concentration. Table VI.D10 shows an example of this calculation for the Figure VI.D9.

Table VI.D10 Example of TIC concentration calculation with the direct TIC methodology

Parameter	Units	Value	Calculated as
Biomass (VSS)	mg VSS/L	1000	Measured
Experimental OUR_{MAX}	mg O_2/L/min	0.5	Measured
Specific OUR_{MAX}	g O_2/g VSS/ min	0.50	Exp OUR_{MAX} / Solids
S_O	Mg O_2/L	5.00	Measured
OUR_{MAX} (*)	g O_2/g VSS/ min	0.57	Specific $OUR_{MAX} \cdot (K_O + S_O)/S_O$
OUR_{END} (mg O_2/L/min)	mg O_2/L/min	0.0153	Measured
CPR_{END} (mmol CO_2/min)	mmol CO_2/L/min	4.3E-04	$OUR_{END} \cdot \gamma_X/8$
k_La_{O2}	1/min	0.25	Measured
k_La_{CO2}	1/min	0.23	$0.91 \cdot k_La_{O2}$
$TIC_{PRESENT}$	mmol CO_2/L	1.9E-03	CPR_{END}/k_La_{CO2}
$NaHCO_{3\ ADDED}$	g $NaHCO_3$	0.03062	Known
$V_{INITIAL}$	L	0.95	Measured
TIC CONCENTRATION	mmol CO_2/L	0.39	$(TIC_{ADDED}/84 \cdot 1000 + TIC_{PRESENT})/V_{INITIAL}$

(*) OUR_{MAX} is recalculated considering oxygen limitations with K_O = 0.74 mg O_2/L (see Chapter VI.C)

Five points were obtained using the methodology of direct TIC calculation proposed in this section. These points are plotted below in Figure VI.D10 as triangle points.

VI.D.4.4 OUR_{MAX} versus TIC: KINETICS ASSESSMENT

Figure VI.D10 shows the profile of OUR_{MAX} as a function of the TIC concentration. As can be observed the profile obtained agrees with the classical substrate limitation profile. In addition, it was experimentally observed that the limitation started at values lower than 3 mM TIC which is a much higher value than the one proposed by ASM2 (Henze *et al.*, 2000), i.e.K_{ALK} = 0.5 mmol HCO_3^-/L

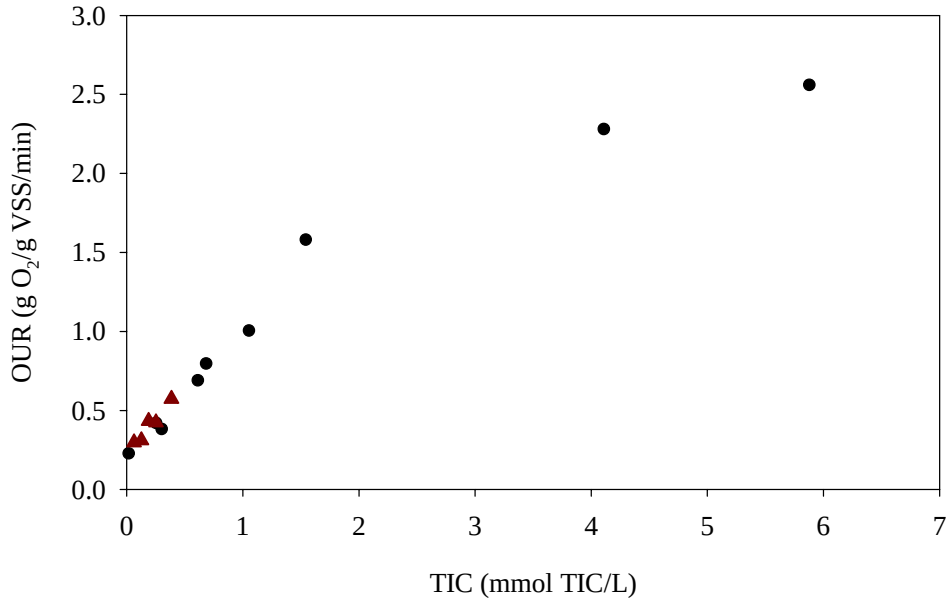

Figure VI.D10 OURMAX vs TIC for experiments VI.D6 (circles) and experiments VI.D7 (triangles)

The experimental results were fitted to the most common limitation equation: Monod kinetics [eq. VI.D11], however the results are not as good as expected (see Figure VI.D11 –solid line).

$$OUR = OUR_{MAX} \cdot \frac{TIC}{K_{TIC} + TIC} \qquad \text{(VI.D11)}$$

Although the fitting seems to describe reasonably good the experimental data in the measured range of TIC, the maximum rate is overestimated (see Table VI.D9). Moreover, the data does not seem to pass through origin which is in discrepancy with Monod prediction. At this point, several other kinetic factors were tested (results not shown). The most plausible results were obtained with a first order kinetics (i.e. Tessier kinetics) [eq. VI.D12].

$$OUR = OUR_{MAX} \cdot \left(1 - e^{-TIC \cdot K_{TIC}}\right) \qquad \text{(VI.D12)}$$

The Tessier profile with the optimum profiles is plotted on Figure VI.D11 (dash-dotted line). Nevertheless, the results of this kinetics were not completely satisfactory, since it also predicts that the experimental data should pass trough origin. The optimum parameters are depicted on Table VI.D11.

Table VI.D11 Parameter estimation results for Monod and first order kinetics

MONOD KINETICS		
OUR_{MAX}	3.11 ± 0.21	g O_2/g VSS/min
K_{TIC}	1.78 ± 0.27	mM
TESSIER (FIRST ORDER) KINETICS		
OUR_{MAX}	2.39 ± 0.12	g O_2/g VSS/min
K_{TIC}	0.64 ± 0.07	mM

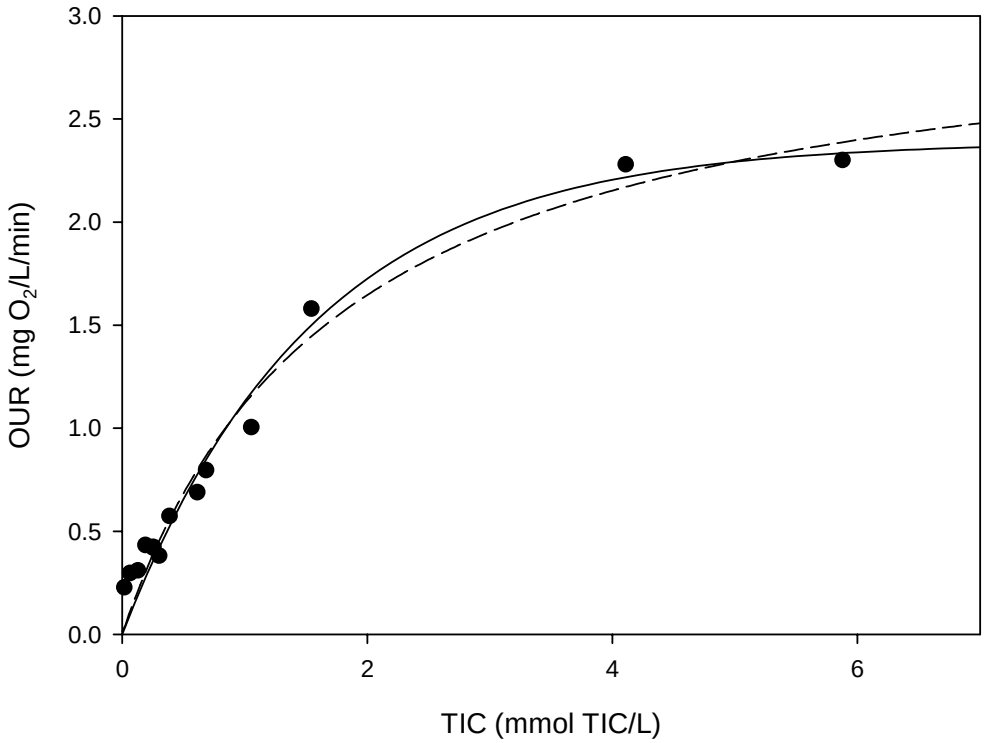

Figure VI.D11 Experimental OUR_{MAX} values (dotted) as a function of TIC. Simulation of Monod kinetics (solid) and Tessier kinetics (dashed)

The main reason for both failures is the fact that the data does not pass through origin. Theoretically, if TIC was not available, the biomass could not grow because it would not have the carbon source. There are some considerations to do at this point:

- According to equation VI.D9 it is impossible to obtain a system without inorganic carbon with mixed cultures because the heterotrophic fraction would always produce some CO_2 (which is characteristic of biomass activity).

- The main explanation for this result should be experimental since obtaining reliable TIC measurements in such a low values is difficult.

- In addition, in a scenario without CO_2, the biomass could use possible COD traces. Clark and Schmidt (1967) demonstrated that AOB from the genus *Nitrosomonas* and NOB from the genus *Nitrobacter* were capable of growing mixotrophically with ammonia or nitrite as electron donors and with a combination of carbon dioxide and organic compounds as carbon source (Dworkin, 2001). This could mean that nitrifying sludge could survive with only organic carbon source. Watson *et al.* (1989) pointed out that organic was not inhibitor, but speeded up the growth of *Nitrobacter Winogradski*. Recently, Perez (2002) and Daims *et al.*, (2000, 2001) showed that in nitrifying sludge NOB biomass could fix CO_2 simultaneously to pyruvate uptake.

In addition, the fact that NOB biomass is not TIC limited in this range of concentrations should also be considered. This could be the reason for observing an intercept higher than zero. However, OUR should not be observed at extremely low CO_2 concentrations (close to zero) since AOB limitation implies very slow nitrite production and, then, nitratation should not take place. In any case, if NOB was not limited, the system should be fitted to equation VI.D13: a modified Monod kinetics, which includes an intercept value (the constant OUR_{MAX} due to NOB value).

$$OUR = OUR_{MAX}(0) + OUR_{MAX} \cdot \frac{TIC}{K_{TIC} + TIC} \quad \text{(VI.D13)}$$

Figure VI.D12 (dashed line) and Table VI.D12 show the parameter estimation results using equation VI.D13. Although the OUR values at low TIC concentrations were correctly predicted, the value of OUR_{MAX} was overestimated using this equation and the fitting could not be considered acceptable. ASM2 (Henze *et al.*, 2000) predicts a Monod kinetics with 0.5 mM HCO_3^-/L of semisaturation constant. This value is rather lower to the value found when fitting Monod kinetics to the experimental data (i.e. 1.78 mM).

On the other hand, Wett and Rauch (2002) also found that the kinetics of carbon limitation do not correspond to Monod kinetics. According to their simulations and experiments with rejection-water treatment, the function describing the influence of HCO_3^- was sigmoidal [eq. VI.D14] with k=50 and a = 10. This equation was also fitted to the experimental results and the fits obtained were very satisfactory as can be observed in Figure VI.D12 (solid line).

$$OUR = OURr_{MAX} \cdot \frac{e^{\frac{TIC-a}{b}}}{1 + e^{\frac{TIC-a}{b}}} \quad \text{(VI.D14)}$$

Table VI.D12 Parameter estimation results for Monod and first order kinetics

MODIFIED MONOD KINETICS		
OUR(0)	0.15 ± 0.06	g O_2/g VSS/min
OUR_{MAX}	3.3 ± 0.3	g O_2/g VSS/min
K_{TIC}	2.5 ± 0.5	mM
SIGMOIDAL KINETICS		
OUR_{MAX}	2.30 ± 0.12	g O_2/g VSS/min
k	1.11 ± 0.07	mM
a	0.57± 0.1	mM

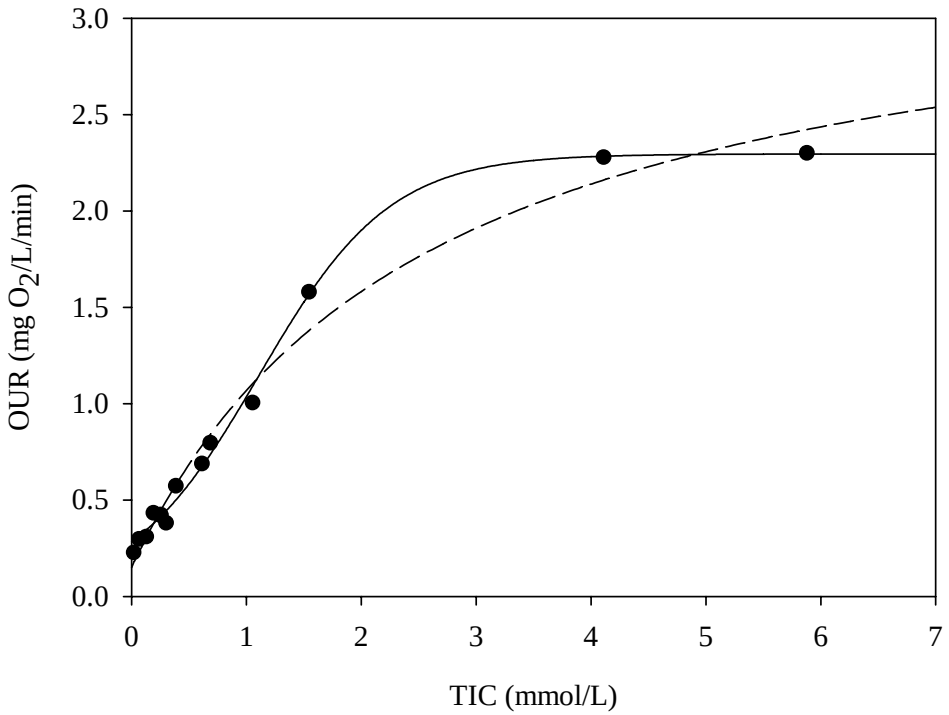

Figure VI.D12 Experimental OUR_{MAX} values (dotted) as a function of TIC. Simulation of modified Monod kinetics (dashed) and sigmoidal kinetics (solid)

As can be observed, the sigmoidal kinetics proposed by Wett and Rauch (2002) described accurately the experimental results obtained, though the parameter estimation values obtained in this thesis are very different to the ones they obtained. Moreover, this kinetics can be too specific for these particular experiments since the sigmoidal factor does not have any known scientific basis.

VI.D.4.5 HPR_{MAX} vs TIC

One of the main advantages of using titrimetry for nitrification monitoring is that it is possible to distinguish between nitritation and nitratation since the latter has no effect on pH. Hence, the evolution of HPR_{MAX} vs TIC is an indicator of the limitation effect on AOB population, without the effect of NOB. Figure VI.D13 shows the evolution of HPR versus TIC in one of the experiments VI.D6 (Table VI.D6). The experiment depicted was one with a low initial bicarbonate pulse: 0.26 mM. The HPR profile obtained is proportional to the OUR profile due to the nitritation since both are an indirect measurement of the nitritation rate.

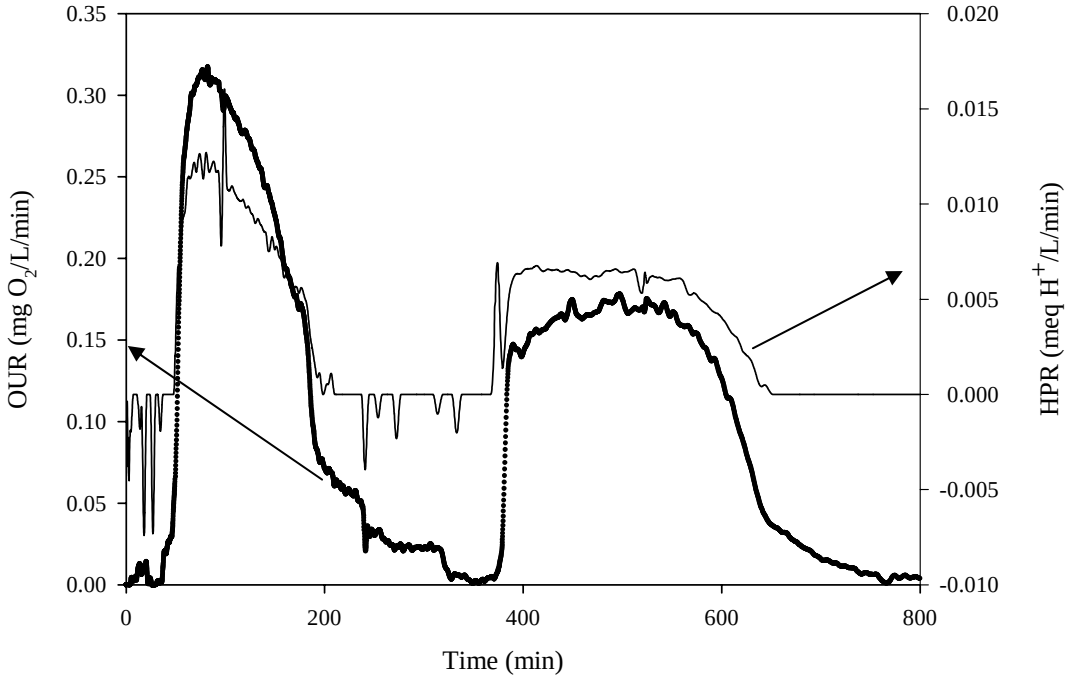

Figure VI.D13 Experimental OUR (dotted) and HPR (solid) profiles for a low initial TIC concentration in one of the experiments VI.D6.

The value of HPR_{MAX} for each experiment was obtained as the difference between the total HPR value and the HPR value owe to the stripping. Actually, the stripping effect was only observed in experiments with high bicarbonate concentration. Figure VI.D14 shows the profiles of HPR_{MAX} vs TIC. The value of HPR_{MAX} has also been corrected for oxygen limitation likewise OUR (see Figure VI.D10). The values of HPR^{MAX} could only be calculated in the set of experiments VI.D6 where the stripping effect on HPR could be reliably distinguished form the HPR due to nitritation.

As can be observed, both Monod and Tessier kinetics described reasonably well the experimental values obtained. Table VI.D13 shows the estimated parameters. In the case of Monod, the estimated value of the affinity constant is somehow lower than the one experimentally observed with OUR (around 1mM). In any case, The TIC limitation effect can be also clearly seen with HPR. Hence, it confirms the observed TIC limitation on AOB observed with OUR.

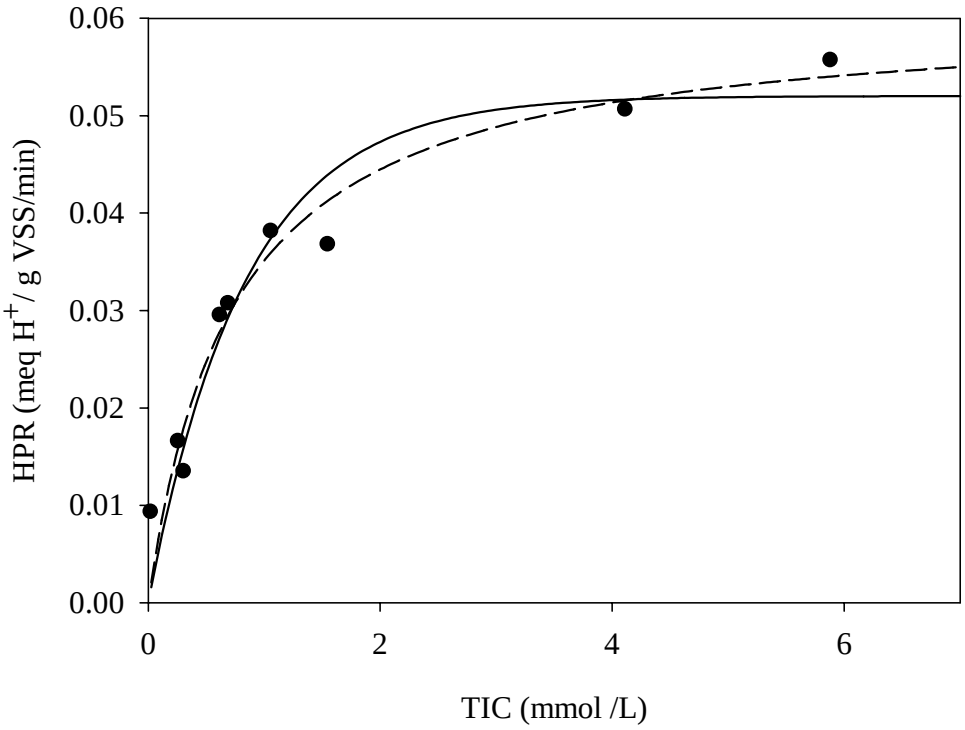

Figure VI.D14 Experimental HPR_{MAX} vs TIC (dotted), Monod kinetics (dashed) and Tessier kinetics (solid).

Table VI.D13 Parameter estimation results for HPR_{MAX} vs TIC

MONOD KINETICS		
HPR_{MAX}	0.061 ± 0.004	meq H^+ /g VSS/min
K_{TIC}	0.73 ± 0.15	mM
TESSIER KINETICS		
HPR_{MAX}	0.052 ± 0.003	meq H^+ /g VSS/min
K_{TIC}	1.20 ± 0.20	Mm

VI.D.5 Significance of the results obtained

The minimum value of TIC where no limitations occur estimated in this chapter (around 4 mM) is noticeably higher than the one previously expected. For instance, ASM2 (Henze *et al.*, 2000), proposes an alkalinity affinity constant of 0.5 mmol HCO_3^-/L. Hence, carbon limitation with conventional air (with 0.036 % CO_2) could be observed. Experiment VI.D9 (Table VI.D14) was conducted to prove that the nitrifying system could be carbon limited with conventional aeration.

Table VI.D14 Experiment VI.D8

EXPERIMENT VI.D9	Carbon limitation with conventional aeration
Equipment	LFS respirometer (V_0 = 0.95 L)
pH	7.5
Temperature	25 ºC
Acid used	HCl (0.5 M)
Pulses	2 · 10 mg N-$NH4^+$
	0.5 g $NaHCO_3$

The system was left overnight with conventional aeration until it reached steady state conditions. Then, a pulse of N as ammonium was added and carbon limitations were observed since the OUR_{MAX} obtained was lower than expected and the consuming time was more than 300 minutes which is certainly a long time for the nitrifying system used in this chapter.

Then, another pulse of N was added and when the maximum rate was reached a pulse of bicarbonate was added. As can be observed in Figure VI.D14, the OUR_{MAX} increased immediately after pulse of bicarbonate was added. Moreover, acid dosage started together with the CO_2 stripping process.

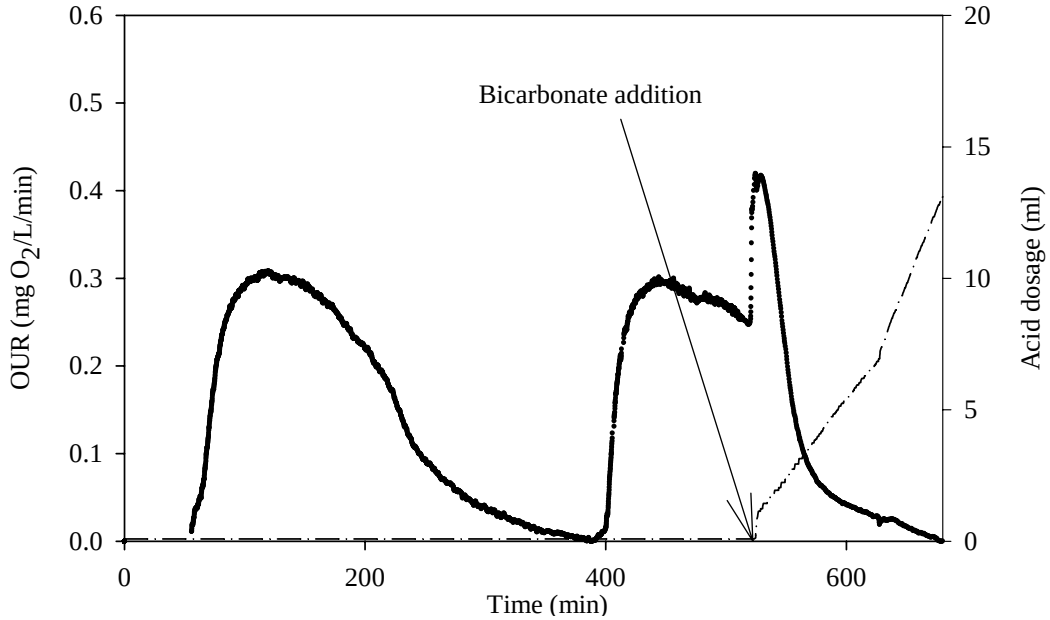

Figure VI.D14 Profiles obtained in experiment VI.D8. Experimental OUR (dotted) and accumulated acid (dash-dotted).

CHAPTER VI.D CONCLUSIONS

- This chapter demonstrates that the nitrification process can be limited with a lack of inorganic carbon.
- However, it seems that this limitation is stronger on the nitritation process than on the nitratation. In fact, the range of TIC concentration where nitratation is limited is so low that it is difficult to reach in an aerobic bioreactor (where CO_2 is produced).
- It was experimentally observed that the limitation started at values lower than 3 mM TIC which is a much higher value than the one proposed by ASM2 (Henze *et al.*, 2000), i.e. K_{ALK} = 0.5 mmol HCO_3^-/L.
- The values of the nitrification rate (measured as OUR) versus TIC concentration could be fitted to a classical Monod and Tessier kinetics. These fittings though successfully described the experimental observations in the measured range could be improved.
- A sigmoidal equation proposed by Wett and Rauch (2002) described successfully the experimental results. However, this expression includes an extra parameter.
- The values of the nitratation rate (measured as OUR with nitrite addition) versus TIC concentration showed that this process is not influenced by the TIC concentration, even at very low TIC values.
- The values of the nitritation rate (measured as HPR) versus TIC concentration confirmed the observed TIC limitation. This limitation could be also described using either Monod or Tessier kinetics.